mathematics

MDPI

Article

Optimal Strategy for Comfort-Based Home Energy Management System Considering Impact of Battery Degradation Cost Model

Binghui Han [1], Younes Zahraoui [2], Marizan Mubin [1,*], Saad Mekhilef [1,3,4], Mehdi Seyedmahmoudian [3] and Alex Stojcevski [3]

[1] Power Electronics and Renewable Energy Research Laboratory (PEARL), Department of Electrical Engineering, Faculty of Engineering, University of Malaya, Kuala Lumpur 50603, Malaysia
[2] FinEst Centre for Smart Cities, Tallinn University of Technology, Ehitajate tee 5, 19086 Tallinn, Estonia
[3] School of Software and Electrical Engineering, Faculty of Science, Engineering and Technology, Swinburne University of Technology, Victoria, VIC 3122, Australia
[4] Institute of Sustainable Energy, Universiti Tenaga Nasional (The National Energy University), Jalan Ikram-Uniten, Kajang 43000, Malaysia
* Correspondence: marizan@um.edu.my

Abstract: With the deployment of renewable energy generation, home energy storage systems (HESSs), and plug-in electric vehicles (PEVs), home energy management systems (HEMSs) are critical for end users to improve the increasingly complicated energy production and consumption in the home. However, few of the previous works study the impact of different models of battery degradation cost in the optimization strategy of a comfort-based HEMS framework. In this paper, a novel scheduling algorithm based on a mixed-integer programming (MIP) model is proposed for the HEMS. Total cost minimization, peak load shifting, and residents' thermal comfort satisfaction are combined and considered in the optimal scheduling algorithm. The impact of battery degradation costs on the charging and discharging strategy of HESS and PEV is also compared and discussed in this case study. This case study shows that the proposed optimal algorithm of HEMS not only flattens the peak load and satisfies the thermal comfort of residents but also has better flexibility and economic advantages, reducing the electricity cost by 30.84% and total cost by 24.16%. The sensitivity analysis of the parameters for the charging and discharging strategy also guarantees the lowest cost and prolongs the service life of the battery.

Keywords: optimization algorithm; home energy management system; degradation cost; thermal comfort; peak load shifting

MSC: 49-11

check for updates

Citation: Han, B.; Zahraoui, Y.; Mubin, M.; Mekhilef, S.; Seyedmahmoudian, M.; Stojcevski, A. Optimal Strategy for Comfort-Based Home Energy Management System Considering Impact of Battery Degradation Cost Model. *Mathematics* **2023**, *11*, 1333. https://doi.org/10.3390/math11061333

Academic Editors: Zhanybai T. Zhusubaliyev and Janez Žerovnik

Received: 28 January 2023
Revised: 21 February 2023
Accepted: 3 March 2023
Published: 9 March 2023

Copyright: © 2023 by the authors. Licensee MDPI, Basel, Switzerland. This article is an open access article distributed under the terms and conditions of the Creative Commons Attribution (CC BY) license (https://creativecommons.org/licenses/by/4.0/).

1. Introduction

Society is facing many issues, including energy shortage and environmental pollution caused by fossil fuels. As a result, renewable energy sources (RESs) have been applied in an increasingly great amount around the world since the first energy crisis, which led to the power grid transiting from a traditional centralized grid to distributed smart grid (SG) [1,2]. However, the deployment of RESs in power systems may create new peaks in the energy system load profile by the volatile and intermittent nature or be interrupted or damaged during natural disasters and faults, which affects the stability of the power grid [3,4].

As shown in Figure 1, the electrical energy usage of residents has increased dramatically to over double times from 1990 to 2020 and is responsible for 27.6% of world electricity final consumption in 2020 [5]. In order to avoid overload due to RESs generation in the power system and afford the rapid increase in different household appliances, home micro-grids (H-MGs) integrating residential small-scale RESs generations such as rooftop

photovoltaic (PV) panels or small wind turbines have been proposed and attracted the attention of many researchers in this field [6].

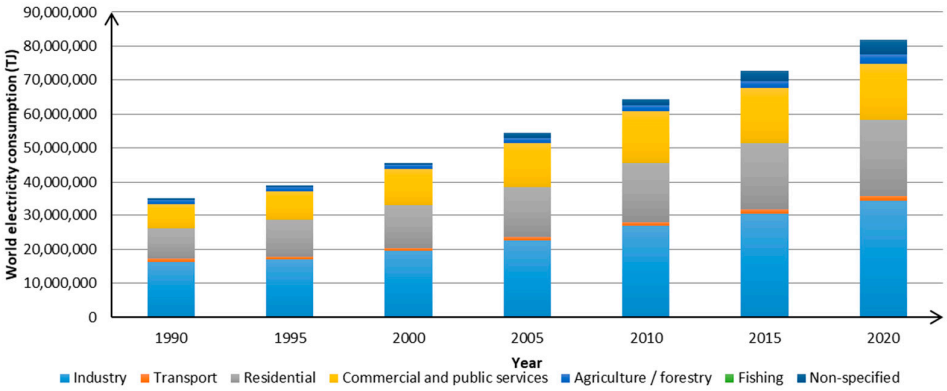


Figure 1. Global electricity consumption by sector from 1990 to 2020 [5].

On the other hand, the development of SG makes the utilities able to offer demand response (DR) programs, e.g., time-dependent rates or financial incentives to users, especially residents, and motivate them to change their consumption patterns according to time-based electricity pricing such as time-of-use (TOU) [7], critical peak pricing (CPP) [8], inclining block rates (IBR) [9], and real-time pricing (RTP) [9,10]. However, these methods can also increase the complexity of energy management in residential buildings. As a result, it is necessary to implement smart energy management at home to reduce power consumption and cost.

A home energy management system (HEMS) can be defined as a system that improves a home's overall energy production and consumption efficiency by controlling and scheduling the generation and consumption of various home appliances [11]. The structure of HEMSs has gradually formed since 1979 and was developed from early analog systems with limited application to modern modular smart systems equipped many extra appliances such as PV panels, home energy storage systems (HESSs), or plug-in electric vehicles (PEVs) [12]. The most important incentive for the prosumers to integrate PV panels is to reduce the electrical energy cost of their home, improve the efficiency of energy usage, and reduce the demand peaks in the PV-integrated HEMSs [13]. Since PEVs not only meet the traffic needs of residents but also provide emergency power for other household loads, extensive research has been undertaken on PEVs to reduce global pollution and improve the stability and efficiency of H-MG energy [14,15].

Except for the architecture development process of HEMSs discussed above, research about scheduling objectives has also been expended in the HEMS field. For example, early studies mainly focused on reducing electricity costs since authors assumed the main reason for deploying HEMS in the home is reducing the electricity cost [16,17]. Recently, besides electricity costs minimization [18–24], research has also been related to battery degradation cost minimization [18], self-scheduling between the grid, RESs generators and loads [25,26], total profit maximization [7,27], cost minimization of the power generation from multiple sources [28], and the running costs minimization [29,30].

However, the excessive reduction in energy costs may lead to discomfort for the users, which prevents residents from participating in the DR program [31]. In addition, the stability between the main grid and H-MGs also needs to consider the expansion of the deployment scale of RESs in residential buildings. As a result, more objectives, such as user comfort load and profiling, have been added to HEMSs. For example, to improve the users' participation in DR projects, there are several methods to enhance user comfort by using HEMS. Among them, the studies about maximizing the comfort factor include the thermal comfort of heating, ventilation, and air conditioning system [18,31], visual comfort of the lighting system [31], suitable load shifting [32], and quick response [19]. Other works also mentioned discomfort minimization, such as thermal discomfort of air conditioner and

domestic hot water [33], waiting for time [18], and unreasonable load shifting [34]. As for load profiling, there are six different strategies, i.e., peak shaving, valley filling, strategic conservation, load shifting, strategic growth, and flexible load shape [23,35–37]. In HEMSs, the methods of load profiling mainly include load peak minimization [15,23], peak-to-average ratio (PAR) reduction [18,38], self-consumption [27], and energy balance [39].

As shown above, there have been many articles about HEMSs. However, few of the above works combined the total cost, load profiling, and user comfort together. In addition, the impact of a different battery degradation cost model on the charging and discharging strategy of HESSs and PEVs in HEMS frameworks also needs more investment. In this paper, a novel mixed integer programming (MIP) model scheme is developed for the HEMS of a smart home integrating three types of domestic appliances, the PV panel, HESS, and PEV.

The objective is to minimize the total cost of the house, including the electricity cost of different types of home appliances and the degradation costs of HESS and PEV, considering RTP and technical constraints. Linear and nonlinear continuous models of air conditioning (AC) and electric water heater (EWH) are formulated, respectively, to satisfy the thermal comfort of the residents. To rationally simulate the degradation costs of HESS and PEV, a simple quadratic model and complex reciprocal model (investment cost of batteries are also included) for batteries of the HESS and EV are taken into account in the HEMS charging and discharging scheduling strategy, respectively, as a comparison of the impact of the same baseline of the degradation costs. The main contributions of this work are listed as follows:

- A mixed objective MIP model of HEMS is formulated to minimize household energy consumption costs and satisfy residents' thermal comfort in daily life by integrating the PV panel, HESS, and PEV, keeping load profiling to the limitation of the utility and combining the users' comfort requirements of both AC and EWH in the framework;
- Two types of battery degradation costs for the HESS and PEV are taken into account in the battery charging and discharging scheduling strategy, considering the impact of RTP and technical constraints. These additions not only guarantee the lowest cost and user's comfort but also manage the energy transaction reasonably between the residence and utility and prolong the service life of the batteries.

The rest of this paper is organized as follows. In Section 2, the total structure and the model of each part of the HEMS are formulated. Then, Section 3 introduces the scheduling objective and proposes the MIP method to solve the optimization problem. Results and discussion of numerical simulation case studies and convergence analyses are elucidated in Section 4. Finally, our conclusions are presented in Section 5.

2. System Modeling

In this paper, the calculated time horizon is set to 24 h, and the time interval Δt is set to 15 min. The total number of time interval is $T = 96$ ($T = 24\ h/\Delta t$). The HEMS layout, which is considered in this paper, is shown in Figure 2. The system is a smart home which is equipped with PV panels, a HESS, a PEV, the utility, a central controller, and three types of home appliances, i.e., entertainment appliances (EAs), constrained appliances (CAs), and schedulable appliances (SAs). Theses equipment are introduced in detail below.

2.1. PV Panels

It is considered that the HEMS has a PV system which can supply the home appliances associated with the power grid. The input power of the PV panels is considered as follows:

$$P_{PV}^{max} = \eta_{PV} S_C A_{PV} Q_{sun} \quad (1)$$

As shown in (1), the PV system is assumed to be a maximum power point tracking system, which guarantees that maximum nominal power P_{PV}^{max} is obtained [40]. The solar irradiance Q_{sun} (the power per unit area) is a function of sun distance, the solar cycle, tile angle of PV surface, and weather condition [41].

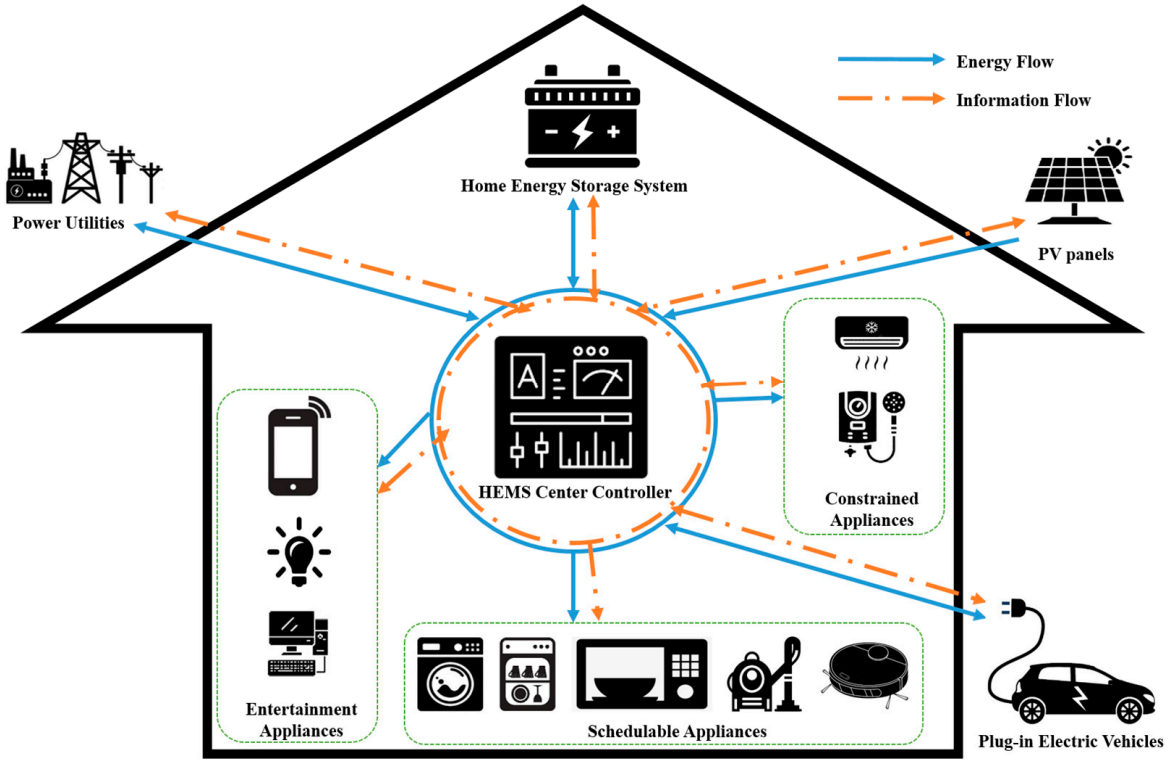


Figure 2. Layout of the home energy management system.

However, the PV output power P_{PV} is capped by its maximum nominal power P_{PV}^{max}.

$$P_{PV} < P_{PV}^{max} \tag{2}$$

Accordingly, the energy that PV panels generated in each period is calculated based on the following relation:

$$E_{PV} = P_{PV}\Delta t \tag{3}$$

2.2. Home Appliances

It is assumed that the home has some of the most commonly used appliances, which are listed in Table 1 [42]. As shown in the first column of Table 1, the appliances are grouped into three categories, namely EA loads, CA loads, and SA loads, to efficiently schedule and obtain better computing experience. The 3rd to 6th columns present the maximum and minimum nominal power and the start and end time of all appliances. The last column of Table 1 shows the running time of the related appliances.

In the presented structure of this paper, EA loads, including smartphone, television, computer, and light, must be fully charged in each time slot because of user's living requests and entertainment needs. CA loads, i.e., AC and EWH, are the appliances that need to be scheduled to satisfy comfort requirements of residents. SA loads, such as washing machine and vacuum cleaner, are scheduled based on the electricity price and other technical constraints of appliances and the utilities. The energy consumption of the appliances can be calculated as follows:

$$E_{load} = \begin{cases} P_{load} num_{load} \Delta t & t_{load}^{start} < t < t_{load}^{end} \\ 0 & \text{Other} \end{cases} \tag{4}$$

$$P_{load}^{min} \leq P_{load} \leq P_{load}^{max} \tag{5}$$

where num_{load} is the number of time intervals that appliances need to fulfill their tasks in a day. The value of num_{load} equals 96 for all EA loads but varies for CA and SA loads

depending on the running time of the appliances. In addition, some SA loads are required to operate more than once a day because of their functionalities. For example, the washing machine has two operation periods every day. The first operation period, namely washing operation, takes one hour of running time. The second operation period is for drying and must be taken after the first operation. So the earliest start time of the second operation of washing machine is 10:00, one hour later than 9:00. The total running time of washing machine is three hours, which means the value of num_{load} of washing machine equals 12. Dishwasher and rice cooker also have two operation periods every day, as shown in Table 1, since they are often used for lunch and dinner.

Table 1. Home appliance parameters.

Category	Appliances	Max Power (kW)	Min Power (kW)	Start Time	End Time	Running Time (h)
EA	Light, Television, Phone, Computer	1	1	8:00	8:00	24
CA	Air Conditioning	3	0	8:00	8:00	24
CA	Electric Water Heater	3.5	0	8:00	8:00	24
SA	Washing Machine	1.5	1.5	9:00	22:00	1
SA	Washing Machine	1.5	1.5	10:00	0:00	2
SA	Dishwasher	1.2	1.2	10:00	15:00	2
SA	Dishwasher	1.2	1.2	18:00	22:00	2
SA	Hairdryer	1.8	1.8	8:00	23:00	0.25
SA	Vacuum Cleaner	1.2	1.2	14:00	18:00	0.5
SA	Rice Cooker	0.8	0.8	10:00	12:00	0.75
SA	Rice Cooker	0.8	0.8	16:00	19:00	0.75
SA	Oven	2	2	10:00	19:00	2
SA	Humidifier	0.15	0.15	8:00	0:00	4
SA	Robot Vacuum Cleaner	0.7	0.7	8:00	0:00	5

Besides the limitation of power, CA loads also need to consider comfort requirements of residents. In this paper, comfort requirements of residents refer to the thermal comfort about the indoor temperature and the hot water temperature. Their formulations and constraints are modeled separately as follows.

The indoor temperature set by the AC is calculated by (6) [43]:

$$T^{in}(t) = T^{in}(t-1) + \alpha\left(T^{out}(t) - T^{in}(t-1)\right) + \beta P_{AC}(t)\Delta t \quad (6)$$

$$T^{in}(t-1) = T^{int}_{in},\ t = 1 \quad (7)$$

$$T^{min}_{AC} \le T^{in}(t) \le T^{max}_{AC} \quad (8)$$

where T^{in} is the scheduled indoor temperature, which has an initial value of T^{int}_{in} and is limited by T^{min}_{AC} and T^{max}_{AC}.

The hot water temperature set by the EWH is calculated by (9).

$$T^{hw}(t) = T^{hw}(t-1)\cdot e^{-(\frac{1}{R'C})\Delta t} + \left[GR'T^{en} + BR'T^{cw} + Q(t)R'\right]\left[1 - e^{-(\frac{1}{R'C})\Delta t}\right] \quad (9)$$

$$T^{hw}(t-1) = T^{int}_{hw},\ t = 1 \quad (10)$$

$$T^{min}_{EWH} \le T^{hw}(t) \le T^{max}_{EWH} \quad (11)$$

where T^{hw} is the scheduled hot water temperature. The energy input rate is expressed as $Q(t) = 3.4121 \times 10^3 \times P_{EWH}(t)$. More detailed explanations for the hot water temperature calculation can be found in [44].

2.3. HESS

As shown in Figure 2, there is a HESS, i.e., a battery, connected to the H-MG, by which the flexibility of HEMS can be enhanced. The operation of the HESS during charging and discharging is modeled as follows [42]:

$$P_{HESS}(t) = P^{ch}_{HESS}(t)u_{HESS}(t) + P^{dis}_{HESS}(t)(1 - u_{HESS}(t)) \tag{12}$$

$$C_{HESS}(t) = C_{HESS}(t-1) + P^{ch}_{HESS}(t)u_{HESS}(t)\Delta t\eta^{ch}_{HESS} + \frac{P^{dis}_{HESS}(t)(1 - u_{HESS}(t))\Delta t}{\eta^{dis}_{HESS}} \tag{13}$$

$$C_{HESS}(t-1) = C^{int}_{HESS},\ t = 1 \tag{14}$$

As shown in (12) and (13), the binary variable u_{HESS} is the running state of HESS, $u_{HESS} = 1$ for charging operation and $u_{HESS} = 0$ for discharging operation. In this model, the power and capacity of the HESS are limited by the maximum charging and discharging power upper and lower limits of capacity of the battery defined by (15), (16), and (17), respectively.

$$0 \le P^{ch}_{HESS}(t)\eta^{ch}_{HESS} \le P^{chmax}_{HESS} \tag{15}$$

$$P^{dismax}_{HESS} \le \frac{P^{dis}_{HESS}(t)}{\eta^{dis}_{HESS}} \le 0 \tag{16}$$

$$0.2C^{max}_{HESS} \le C_{HESS}(t) \le 0.8C^{max}_{HESS} \tag{17}$$

where η^{ch}_{HESS} and η^{dis}_{HESS} are charging and discharging efficiency of the battery used in HESS.

2.4. PEV

When using as a household load, a PEV is like a SA load. When scheduling as energy storage, a PEV is similar to the HESS. The capacity and power of PEV are presented as follows:

$$P_{PEV}(t) = P^{ch}_{PEV}(t)u_{PEV}(t) + P^{dis}_{PEV}(t)(1 - u_{PEV}(t)),\ t \in [t_a,\ t_d) \tag{18}$$

$$C_{PEV}(t) = C_{PEV}(t-1) + P^{ch}_{PEV}(t)u_{PEV}(t)\Delta t\eta^{ch}_{PEV} + \frac{P^{dis}_{PEV}(t)(1 - u_{PEV}(t))\Delta t}{\eta^{dis}_{PEV}},\ t \in [t_a,\ t_d) \tag{19}$$

$$C_{PEV}(t-1) = C^{int}_{PEV},\ t \le t_a \tag{20}$$

where t_a and t_d are the arriving time and department time of the PEV. Additionally, similar to the HESS, the capacity and power constraints of the PEV can be defined as follows:

$$0 \le P^{ch}_{PEV}(t)\eta^{ch}_{PEV} \le P^{chmax}_{PEV},\ t \in [t_a,\ t_d) \tag{21}$$

$$P^{dismax}_{PEV} \le \frac{P^{dis}_{PEV}(t)}{\eta^{dis}_{PEV}} \le 0,\ t \in [t_a,\ n] \tag{22}$$

$$\begin{cases} 0.3C^{max}_{PEV} \le C_{PEV}(t) \le 0.8C^{max}_{PEV} & t \in [t_a,\ t_d - 1) \\ C_{PEV}(t) \ge 0.8C^{max}_{PEV} & t = t_d - 1 \end{cases} \tag{23}$$

2.5. Utility

As discussed in Section 1, the main benefit of the utility of participating in the DR program is load profiling. Since the interaction power between the utility and H-MG P_G is calculated by (24), the peak power constraint can be expressed by (25) to avoid the formation of new peaks during low price periods [42].

$$P_G(t) = P_E(t) + P_{AC}(t) + P_{EWH}(t) + \sum_{s=1}^{S} P_s(t)u_s(t) + P_{HESS}(t) + P_{PEV}(t) - P_{PV}(t) \tag{24}$$

$$P_G(t) \leq P_{DR} \tag{25}$$

where P_{DR} is the maximum power drawn from the utility.

2.6. Central Controller

As shown in Figure 2, the central controller controls and schedules all the home appliances, PV generation, and energy storage of the HESS as well as the power transmitted between the main grid and the H-MG. The main objective of the HEMS in this paper is to minimize the electricity cost and the total cost for the user, which can be calculated in (26) and (27).

$$\text{minCost}(P_G) = \sum_{t=1}^{T} P_G(t) \cdot RTP(t) \cdot \Delta t \tag{26}$$

$$\text{minCost}_{\text{total}(P_G)} = \sum_{t=1}^{T} P_G(t) \cdot RTP(t) \cdot \Delta t + \cos t^{deg}_{HESS,\ PEV}(t) \tag{27}$$

where $PRT(t)$ is the real-time price of the utility in time t, and $\cos t_{deg}(t)$ is the function of the degradation costs of the HESS and PEV.

3. Proposed Method

To decrease the operation cost of the system, reduce battery degradation, and study the impact of different models of HESS and PEV rationally, both quadratic model and reciprocal model for batteries of the HESS and PEV are taken into account in the HEMS charging and discharging scheduling strategy, respectively, as a comparison of the impact of the same baseline of the degradation costs.

3.1. Quadratic Model of the Battery Degradation

To simplify the analysis, the degradation cost of the HESS and PEV can be approximated with a quadratic function as follows:

$$\cos t^{deg}_{HESS,\ PEV}(t) = \gamma \cdot \left(P^{dis}_{HESS,\ PEV} - P^{ch}_{HESS,\ PEV}\right)^2 \tag{28}$$

where the parameter γ equals 0.0625 according to [45].

3.2. Reciprocal Model of the Battery Degradation

The reciprocal model of degradation for batteries of the HESS and PEV can be defined as follows [10,46]:

$$RTP^{deg}_{HESS,\ PEV} = \theta \cdot \frac{Rep_{HESS,\ PEV}}{L_{HESS,\ PEV}\eta_{HESS,\ PEV}} \tag{29}$$

$$L_{HESS,\ PEV} = Cyc_{HESS,\ PEV} \cdot C^{max}_{HESS,PEV} \cdot DoD_{HESS,\ PEV} \tag{30}$$

$$\cos t^{deg}_{HESS,\ PEV}(t) = RTP^{deg}_{HESS,\ PEV} \cdot \left(P^{dis}_{HESS,\ PEV} - P^{ch}_{HESS,\ PEV}\right) \tag{31}$$

where $RTP^{deg}_{HESS,\ PEV}$ is the real-time cost of the battery degradation of the HESS and PEV that should be added into the buying and selling prices of the power between the main grid and the H-MG. More detailed explanations for the degradation cost calculation can be found in the Nomenclature section.

It should be noted that the investment costs of batteries are also included in the reciprocal degradation cost model, and the degradation cost is not included in the electricity bill. The real-time cost of the battery degradation is used to study the impact of a different model of degradation cost on the charging and discharging strategy of the HESS and PEV rationally. The optimization objective of this paper is to minimize the total cost of the H-MG, which means the sum of the electricity bill and the degradation cost of the HESS and PEV.

3.3. Charging and Discharging Strategy

To minimize the electricity costs and reduce the battery charging and discharging cycles of HESS and PEV, a charging and discharging strategy is proposed for the batteries of HESS and PEV, which separate the operating time of PEV connected to the H-MG into two operation modes.

Specifically, when PEV is connected to the H-MG, the total available time period for charging and discharging $[t_a, t_d)$ is divided into two segments according to the latest time slot during which the PEV must be charged, namely n^{th} time slot, to meet the user's travel requirement. In this strategy, PEV is used as energy storage in $[t_a, n]$ and only as a load in $[n+1, t_d)$. More detailed explanations for the calculation of n can be found in [42].

Based on the value of time slot n and the principle that the PEV and HESS will only discharge when the electricity price is above a certain threshold, the charging and discharging strategy for the batteries of HESS and PEV is shown in Figure 3.

The maximum value of allowable charging and discharging power of HESS and PEV are calculated under battery capacity constraints and presented as follows:

$$P_{HESS}^{chable}(t) = (0.8C_{HESS}^{max} - C_{HESS}(t-1))/\left(\eta_{HESS}^{ch}\Delta t\right) \tag{32}$$

$$P_{HESS}^{disable}(t) = (C_{HESS}(t-1) - 0.2C_{HESS}^{max})\eta_{HESS}^{dis}/\Delta t \tag{33}$$

$$P_{PEV}^{chable}(t) = (0.8C_{PEV}^{max} - C_{PEV}(t-1))/\left(\eta_{PEV}^{ch}\Delta t\right) \tag{34}$$

$$P_{PEV}^{disable}(t) = (C_{PEV}(t-1) - 0.2C_{PEV}^{max})\eta_{PEV}^{dis}/\Delta t \tag{35}$$

where P_{HESS}^{chable}, $P_{HESS}^{disable}$, P_{PEV}^{chable}, and $P_{PEV}^{disable}$ are the maximum chargeable and dischargeable power of HESS and PEV, representatively.

Then, the specific execution steps of the two situations are discussed, respectively.

Situation 1: in this period (i.e., $[t_a, n]$), PEV is similar to the HESS and has the ability to supply the consumption of loads in the H-MG. Its execution steps are as follows:

Step 1. Calculate P1 by (36). P1 is the total energy of H-MG without considering HESS and PEV in the power system.

$$P1(t) = P_E(t) + P_{AC}(t) + P_{EWH}(t) + \sum_{sa=1}^{SA} P_{sa}(t)u_{sa}(t) - P_{PV}(t) \tag{36}$$

Step 2. If $P1(t) > 0$, the total energy of H-MG is insufficient, which means the H-MG needs power supply from the utility or the energy storage device. Both HESS and PEV are available in this situation.

Step 3. If $RTP(t) > RTP_{HESS}^{dis}$, HESS will discharge, and the discharging power and capacity of HESS will be calculated by (37) and (38); otherwise, HESS will take no action:

$$P_{HESS}(t) = -\min\left(P1(t),\ P_{HESS}^{disable}(t),\ \left|P_{HESS}^{dismax}\right|\eta_{HESS}^{dis}\right) \tag{37}$$

$$C_{HESS}(t) = C_{HESS}(t-1) + \frac{P_{HESS}(t)\Delta t}{\eta_{HESS}^{dis}} \tag{38}$$

Step 4. Calculate P2 by (39). P2 is the system energy of H-MG considering the charging and discharging power of HESS in the power system.

$$P2(t) = P1(t) + P_{HESS}(t) \tag{39}$$

Step 5. If $RTP(t) > RTP_{PEV}^{dis}$, PEV will discharge, and the discharging power and capacity of PEV will be calculated by (40) and (41); otherwise, PEV will take no action:

$$P_{PEV}(t) = -\min\left(P2(t),\ P_{PEV}^{disable}(t),\ \left|P_{PEV}^{dismax}\right|\eta_{PEV}^{dis}\right) \tag{40}$$

$$C_{PEV}(t) = C_{PEV}(t-1) + \frac{P_{PEV}(t)\Delta t}{\eta_{PEV}^{dis}} \quad (41)$$

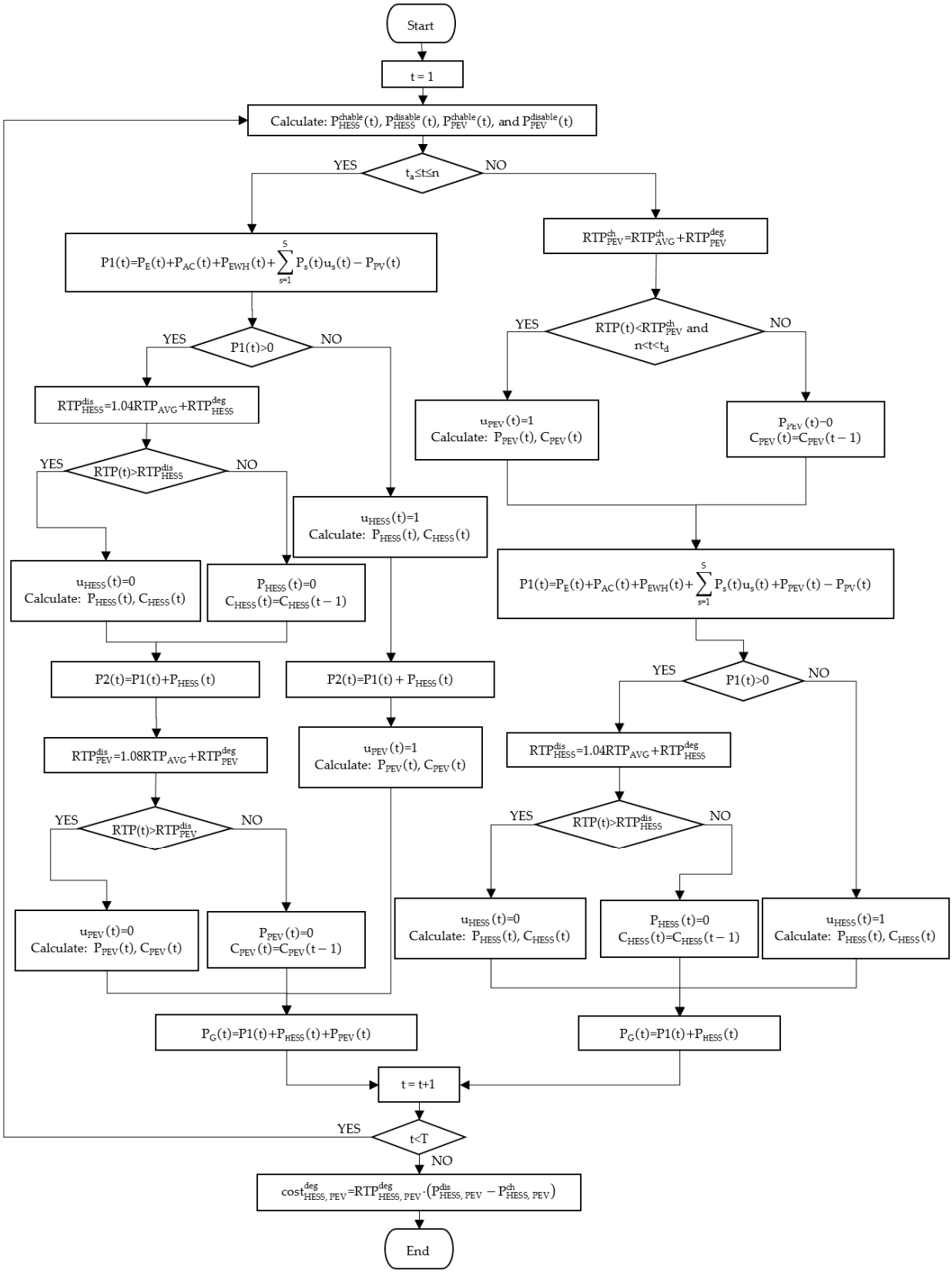


Figure 3. Flow chart of the charging and discharging strategy for the batteries of HESS and PEV.

Step 6. If $P1(t) < 0$, the total energy of H-MG is surplus, which means the extra energy can be injected to the energy storage device, i.e., HESS and PEV, and the charging power and capacity of HESS and PEV will be calculated by (42)–(45):

$$P_{HESS}(t) = \min\left(-P1(t),\ P_{HESS}^{chable}(t),\ P_{HESS}^{chmax}/\eta_{HESS}^{ch}\right) \tag{42}$$

$$C_{HESS}(t) = C_{HESS}(t-1) + P_{HESS}(t)\eta_{HESS}^{ch}\Delta t \tag{43}$$

$$P_{PEV}(t) = \min\left(-P2(t),\ P_{PEV}^{chable}(t),\ P_{PEV}^{chmax}/\eta_{PEV}^{ch}\right) \tag{44}$$

$$C_{PEV}(t) = C_{PEV}(t-1) + P_{PEV}(t)\eta_{PEV}^{ch}\Delta t \tag{45}$$

Step 7. Calculate P_G by (46). P_G is the interaction power between the utility and the H-MG.

$$P_G(t) = P1(t) + P_{HESS}(t) + P_{PEV}(t) \tag{46}$$

Situation 2: in $[1,\ t_a)$ and $(n,\ T]$, PEV is not connected to the H-MG or only used as a load in the H-MG. Its calculation steps are described as follows:

Step 1. If $RTP(t) < RTP_{PEV}^{ch}$ and $n < t < t_d$, PEV will be charged, and the discharging power and capacity of PEV will be calculated by (47); otherwise, PEV will take no action:

$$P_{PEV}(t) = \min\left(P_{temp}(t),\ P_{PEV}^{chable}(t),\ P_{PEV}^{chmax}/\eta_{PEV}^{ch}\right) \tag{47}$$

Step 2. Calculate P1 by (48). P1 is the total energy of H-MG without considering HESS in the power system:

$$P1(t) = P_E(t) + P_{AC}(t) + P_{EWH}(t) + \sum_{sa=1}^{SA} P_{sa}(t)u_{sa}(t) + P_{PEV}(t) - P_{PV}(t) \tag{48}$$

Step 3. If $P1(t) > 0$ and $RTP(t) > RTP_{HESS}^{dis}$, HESS will discharge, and the discharging power and capacity of HESS will be calculated by (37) and (38); otherwise, HESS will take no action.

Step 4. If $P1(t) < 0$, the total energy of H-MG is surplus, and the charging power and capacity of HESS will be calculated by (42) and (43);

Step 5. Calculate P_G by (49).

$$P_G(t) = P1(t) + P_{HESS}(t) \tag{49}$$

3.4. Optimization Algorithms

In this work, we combined the total cost, load profiling, and user comfort together and studied the impact of different models of battery degradation cost in the combined charging and discharging strategy of HESS and PEV in a comprehensive HEMS model. Since the model of AC is a linear function, the model of EWH is a nonlinear reciprocal function, and the model of SA loads has binary variables, a novel MIP algorithm is developed for the HEMS to minimize the total cost of the house considering RTP and thermal comfort of the user.

As shown in Figure 4, firstly, the HEMS reads the meta data for PV and CAs, such as PV generation, RTP, ambient temperature, and hot water usage. Secondly, data about the maximum and minimum power, start and end time, and the total run time of all types of household appliances are read by the HEMS. Then, the consumption of CA and SA loads are optimized and scheduled based on the temperature and technical constraints of appliances. Initial parameters of HESS and PEV and parameters for the degradation cost of batteries are put into the HEMS to calculate the total real-time charging and discharging price. The value of last discharging time slot n is calculated, then. The optimal solution is obtained according to the former optimal scheduling plan of all home appliances and the

proposed charging and discharging strategy of HESS and PEV. Finally, the electricity cost and the total cost of users in daily life are calculated based on the optimal solution.

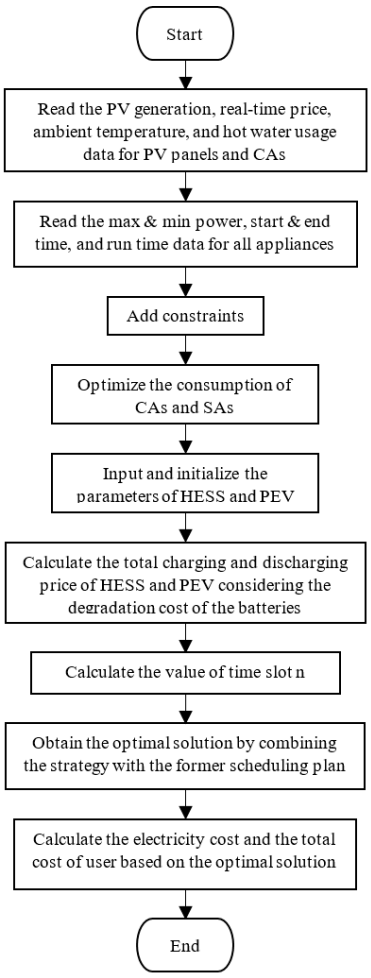


Figure 4. Flow chart of the optimization algorithm for HEMS.

4. Results and Discussion

In this paper, the arriving and departure time of PEV are assumed to be 18:30 and 7:30. Figure 5 shows the PV generation data converted from the PV generation data of the European Network of Transmission System Operators to meet the residence PV generation [42]. Figure 6 depicts the real-time pricing of the utility from the Australian Energy Market Operator [47]. Tables 2 and 3 present the parameters of thermal comfort of the user and batteries of HESS and PEV, respectively [10,42]. The power purchased from the utility is limited to 5 kW [42]. In addition, the outdoor temperature data is taken from [43], and the hot water demand information is taken from [48].

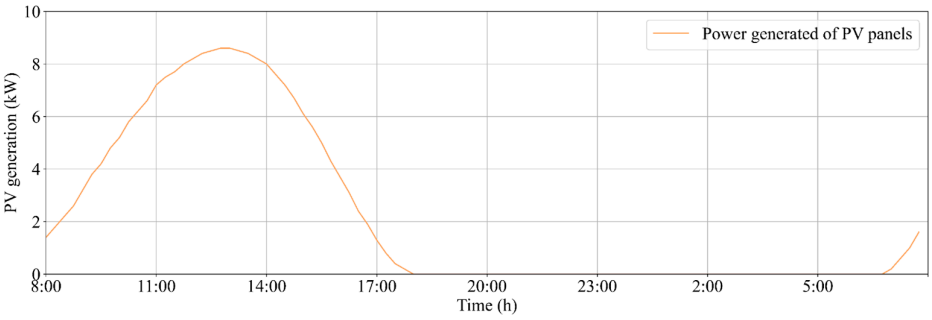


Figure 5. Energy generation of the PV panels.

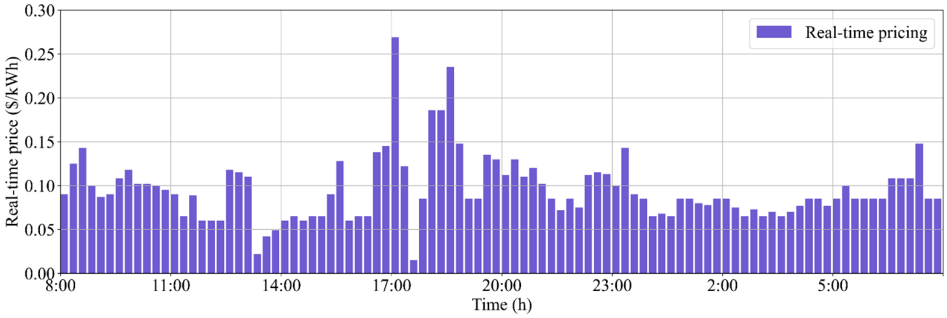


Figure 6. Real-time pricing of the utility.

Table 2. Parameters of thermal comfort of the user.

Parameters for Indoor Temperature Calculation		Parameters for Hot Water Temperature Calculation	
T_{AC}^{max} (°F)	80	T_{EWH}^{max} (°F)	150
T_{AC}^{min} (°F)	73	T_{EWH}^{min} (°F)	120
T_{AC}^{int} (°F)	77	T_{EWH}^{int} (°F)	70
α	0.9	T^{cw} (°F)	70
β	−11	T^{en} (°F)	80

Table 3. Parameters of HESS and PEV.

Parameters for HESS		Parameters for PEV	
C_{HESS}^{max} (kWh)	8	C_{PEV}^{max} (kWh)	30
C_{HESS}^{int} (kWh)	3.5	C_{PEV}^{int} (kWh)	12
P_{HESS}^{chmax} (kW)	3	P_{PEV}^{chmax} (kW)	4
P_{HESS}^{dismax} (kW)	−3	P_{PEV}^{dismax} (kW)	−4
η_{HESS}^{ch} / η_{HESS}^{dis}	0.92	η_{PEV}^{ch} / η_{PEV}^{dis}	0.92
DoD_{HESS} (%)	70	DoD_{PEV} (%)	80
Cyc_{HESS}	1250	Cyc_{PEV}	2000
Rep_{HESS} ($)	695	Rep_{PEV} ($)	2850
RTP_{HESS}^{dis}	$1.04RTP_{AVG}$	RTP_{PEV}^{dis}	$1.08RTP_{AVG}$

The simulation is conducted on a personal computer with IntelCore^{TM} i3 − 4130 CPU @ 3.40 GHz and 16 GB of RAM, running on Windows 10 64-bit education system. Python v.3.9.12 with GLPK v.5.0 and IPOPT v.3.11.1 in the platform pyomo v.6.4.2 is used as the programming and solving platform.

4.1. Appliances Scheduling Results

The simulation results of the optimal scheduling of all the household appliances are presented in Figures 7–9. As shown in Table 2, the indoor temperature (°F) and the hot water temperature (°F) are assigned initial values of 77 and 70 and are limited to vary in intervals of [73, 80] and [120, 150], respectively. The curve in Figure 8a shows the everyday hot water usage. Figures 7 and 8b present that both the indoor and hot water temperatures are within the acceptable temperature limits throughout the whole calculated horizon, illustrating the comfort requirements of the resident are satisfied by the scheduling plan of this work.

Figure 9 depicts the overall optimized scheduling plan of all the domestic appliances, which is well matched with the timetable of all the appliances shown in Table 1. The total power consumption of each time is also matched approximately with the power generation of PV panels (see Figure 5), except the real-time price is very low.

It is worth noting that the scheduling plan in Figure 9 also indicates the necessity to equip a HESS in a PV-integrated H-MG. Since PV panels can only work in the daytime, and their output is highly affected by solar radiation, PV-integrated H-MGs may suffer from

the power excess during the daytime and power shortage at night when supporting the total consumption of the appliances without a HESS connected to the H-MG.

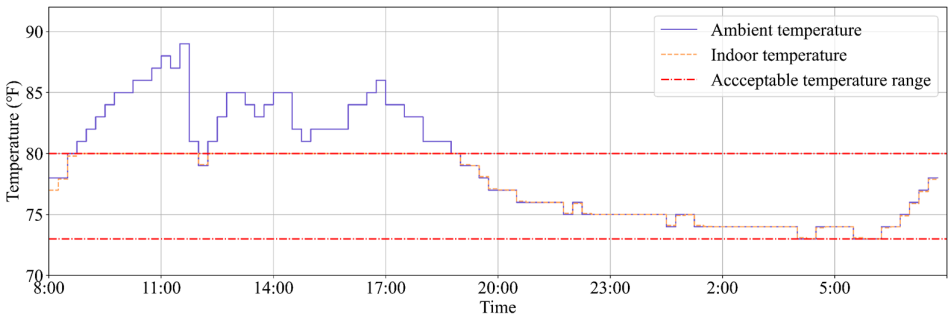


Figure 7. Scheduling results of the air conditioning considering thermal comfort of the residents.

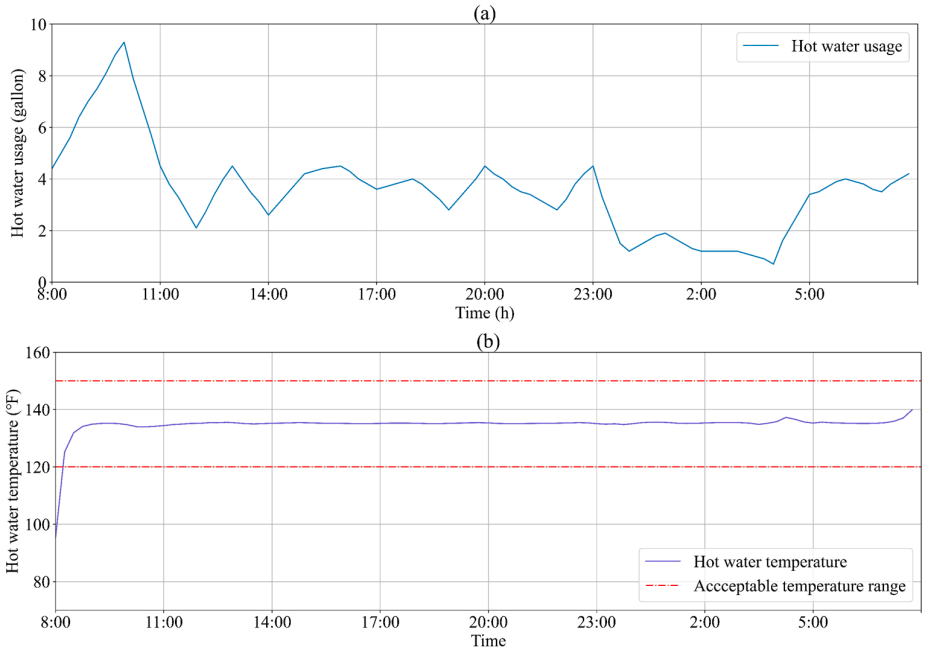


Figure 8. (**a**) Hot water usage and (**b**) scheduling results of the electric water heater considering thermal comfort of the residents.

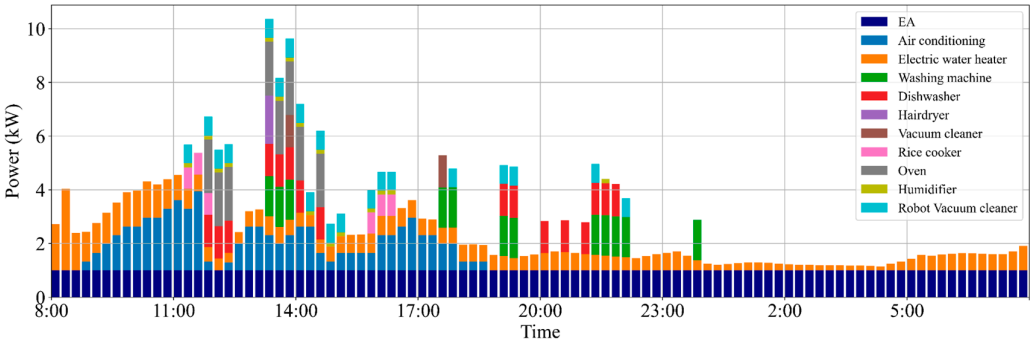


Figure 9. Overall scheduling results of all the home appliances.

4.2. Case Study

To make full use of RESs in the residential buildings and minimize the total cost of the H-MG, different cases are designed to examine the economy of different HEMS, both architectures and optimization algorithms, and the effect of the proposed mode segment

strategy. The impact of two degradation cost models are also compared between the cases. The summary of the results is presented in Table 4.

Table 4. Case comparison results.

Case	Battery Degradation	HESS	PEV	Mode Segment Strategy	Degradation Cost (Cent)	Cost (Cent) (P_sold = 0.5RTP)	Cost_total (Cent) (P_sold = 0.5RTP)
Case 1	Quadratic model	No	No(G2V)	No	28.08	389.78 (100.00%)	417.86 (100.00%)
Case 2		Yes(HESS2H)	No(G2V)	No	37.72	325.60 (83.53%)	363.31 (86.95%)
Case 3		Yes(HESS2H)	Yes(V2H)	No	47.12	271.19 (69.58%)	318.31 (76.18%)
Case 4		Yes(HESS2H)	Yes(V2H)	Yes	47.34	269.58 (69.16%)	316.92 (75.84%)
Case 5	Reciprocal model	No	No(G2V)	No	28.08	389.78 (100.00%)	417.86 (100.00%)
Case 6		Yes(HESS2H)	No(G2V)	No	49.23	328.93 (84.39%)	378.16 (90.50%)
Case 7		Yes(HESS2H)	Yes(V2H)	No	49.88	293.67 (75.34%)	343.56 (82.22%)
Case 8		Yes(HESS2H)	Yes(V2H)	Yes	49.88	276.00 (70.81%)	325.88 (77.99%)

The sixth column of Table 4 shows the total daily battery degradation cost of HESS and PEV. The last two columns of this table present the electricity cost and the total cost (sum of electricity cost and battery degradation cost of HESS and PEV) separately when the price of power sold to the utility is 50% of the buying price of the utility [42].

4.2.1. HEMSs with Quadratic Model of Degradation Cost

In Case 1, which is considered the base case, it is assumed that the smart home is equipped with a PV system but not any HESS. The PEV is in the grid-to-vehicle (G2V) mode with the quadratic degradation cost model. Since the PEV can only be used as a domestic load and meet the travel demand of the residents in the G2V mode, the cost of energy is 3.8978 USD/day, and the total cost is 4.1786 USD/day when the extra energy generated by the PV system is sold to the utility. Load profiles of the home for PEV in the G2V mode and for the interaction power between the utility and the H-MG are shown in Figure 10.

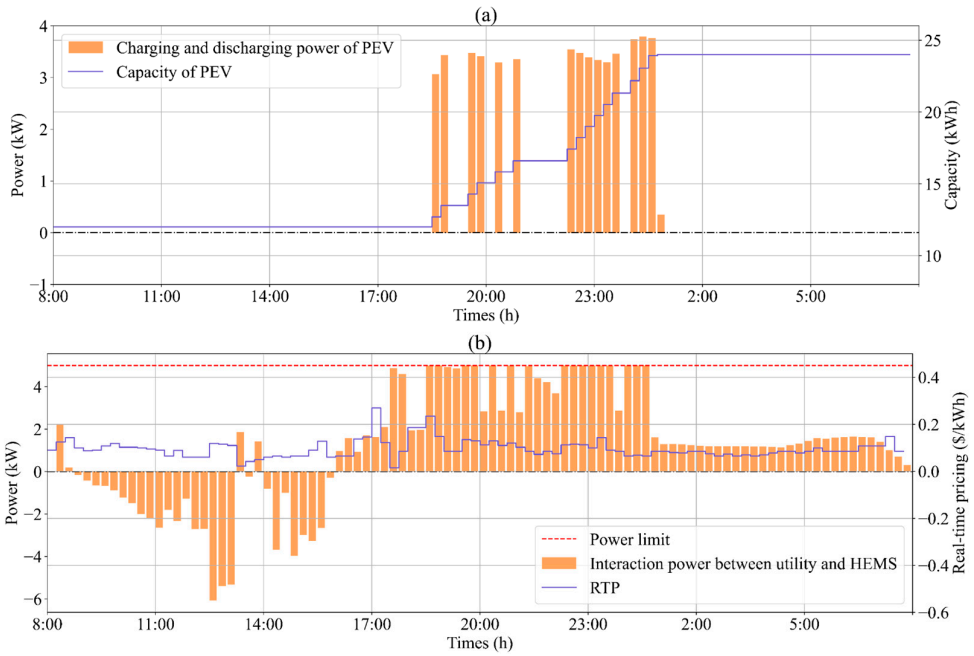


Figure 10. Load profiles for (**a**) PEV in G2V mode and (**b**) H-MG without mode segmentation strategy.

In Case 2, the optimal operation of the PV- and HESS-integrated HEMS is modeled. The HESS is in the HESS-to-home (HESS2H) mode, and PEV is in the G2V mode with

the quadratic degradation cost model. The electricity cost and total cost in this case are 3.2560 USD/day and 3.6331 USD/day when the selling price of energy is 50% of the buying price of the utility. These results show a great reduction in electricity cost in comparison with Case 1, but on the other hand, the degradation cost rises greatly, which depicts the increase in battery operation for the connection of HESS when the charging operation of PEV is the same as the operation of PEV in Case 1. Figure 11 also proves this opinion, which shows load profiles of the home for HESS in HESS2H mode and PEV in G2V mode and for the interaction power between the utility and the H-MG.

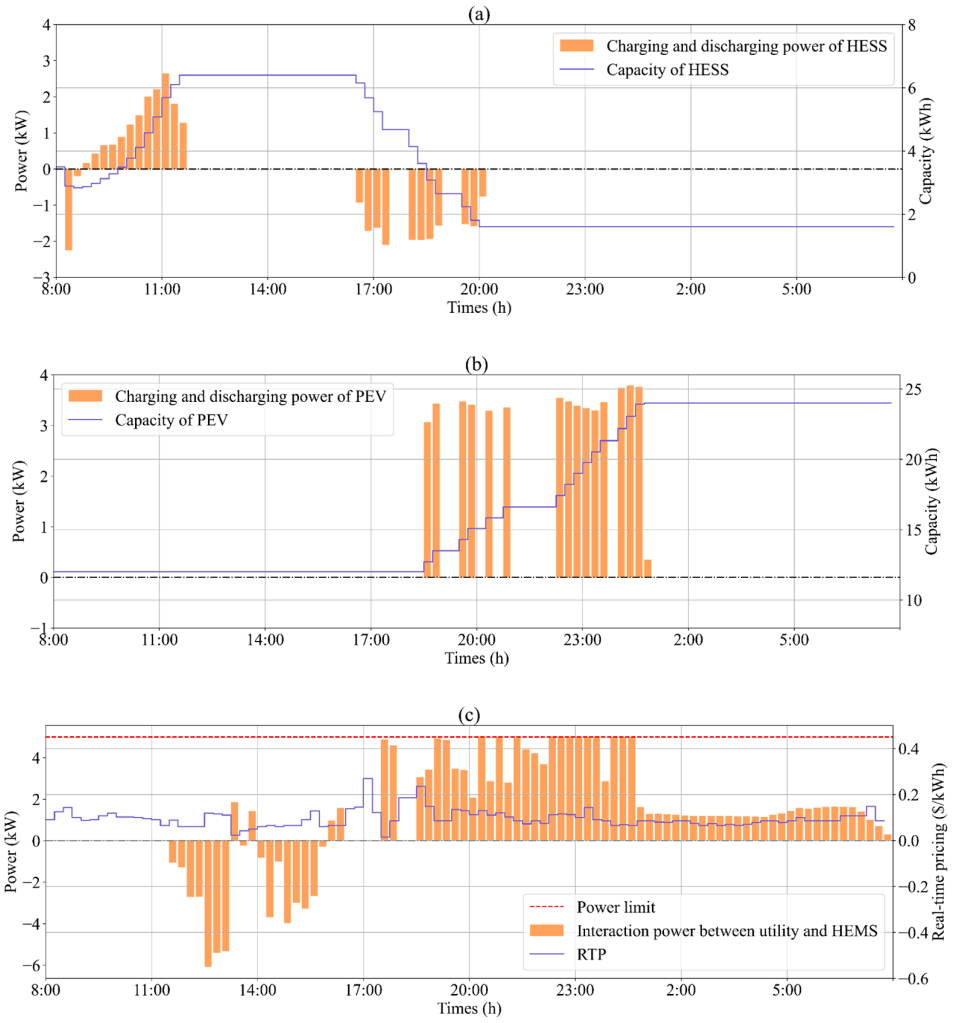


Figure 11. Load profiles for (**a**) HESS in HESS2H mode, (**b**) PEV in G2V mode, and (**c**) H-MG without mode segmentation strategy.

In comparison to Case 2, it is assumed that PEV is in the vehicle-to-home (V2H) mode in Case 3, while other conditions are the same. The PEV in V2H mode can be used as a load and an energy supply device for all other home appliances. In this case, the cost of electricity and total cost are reduced up to 69.58% and 76.18% separately compared with Case 1, and a continuous drop compared with Case 2. Growth of the degradation cost from 0.3772 USD/day to 0.4712 USD/day is seen in Table 4, which matches the increasing changes of the charging and discharging operation shown in Figure 12 in the load profile for PEV in the V2H mode while the operation of HESS is same as the operation of HESS in Case 2.

In Case 4, the proposed battery charging and discharging strategy controlled by the RTP is applied to the PV- and HESS-integrated HEMS considering the degradation cost of

batteries. In this case, the energy cost is 2.6958 USD/day, a 30.84% descent compared to Case 1, and the total cost is 3.1692 USD/day, a 24.16% descent compared to Case 1.

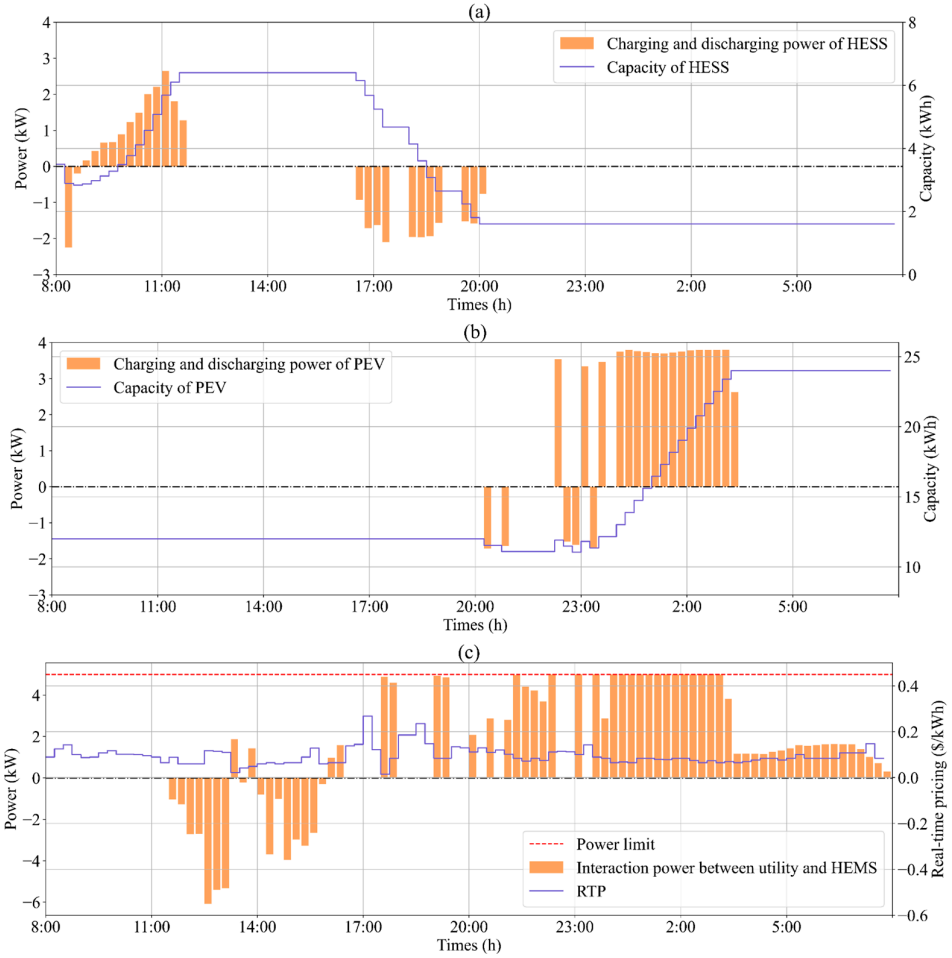


Figure 12. Load profiles for (**a**) HESS in HESS2H mode, (**b**) PEV in V2H mode, and (**c**) H-MG without mode segmentation strategy.

It is noted that there is a slight growth in total daily degradation cost from 0.4712 USD/day in Case 3 to 0.4734 USD/day in Case 4. However, as shown in Figure 13, HESS presents the same load profile for Case 2 and Case 3. The discharging behavior of PEV is also same as the behavior of PEV in Case 3, so it can be seen that this growth is caused by the charging operation of PEV. Since the PEV's charging time is postponed to the early morning compared with Case 3, and considering the relationship of power and capacity shown in (18), (19), (34), and (35), it is revealed that the slight growth of total daily degradation cost is caused by the repeated charging and discharging behavior of PEV in the period of 22:15 to 23:30 in Case 3, which affects the calculation of the dynamic degradation cost by quadratic modeling. Compared with the above cases, the proposed charging and discharging strategy not only achieves the purpose of reducing energy costs but also shifts the charging process of PEV to a more suitable time and avoids the harmful behavior of repeated charging and discharging of the battery in a short period of time, which shows potential in prolonging the service life of the battery.

4.2.2. HEMSs with Reciprocal Model of Degradation Cost

As control groups for the quadratic model of degradation cost, to meet the same baseline of the degradation costs when HESS is not equipped in the home and the PEV only used as a load in Case 1, in reference to the parameter γ in [10], it is assumed that the value of parameter θ equals 0.2919 in the following cases.

In Case 5, which is also considered the base case of the reciprocal model of degradation cost, it is assumed that the smart home is equipped with a PV system but not any HESS. The PEV is in the G2V mode with the reciprocal degradation cost model. The electricity cost, total cost, and load profiles for PEV and H-MG are the same as Case 1.

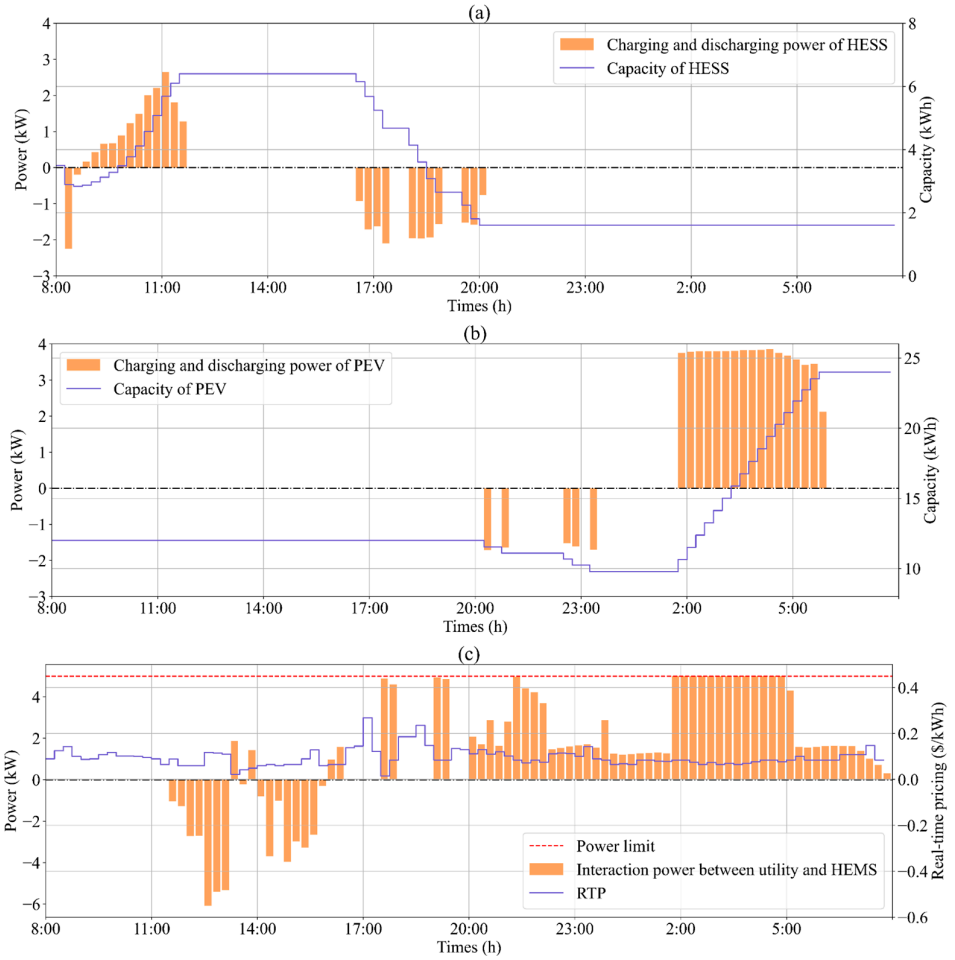


Figure 13. Load profiles for (**a**) HESS in HESS2H mode, (**b**) PEV in V2H mode, and (**c**) H-MG combined mode segmentation strategy.

Load profiles for HESS in the HESS2H mode, PEV in the G2V mode, and energy interactions in H-MG of Case 6 are presented in Figure 14. PEV's load profile in Case 6 is same as the profiles of PEV in Cases 1, 2, and 5, as shown in Figure 14b. Compared with Case 2, HESS in Case 6 shows the same charging operation but a longer discharging time. As shown in Figure 14d, the total discharging RTP of HESS with the reciprocal model is always higher than the total discharging RTP of HESS with the quadratic model and has less of a chance to be greater than the RTP of the utility, which affects the final behavior of HESS of the proposed charging and discharging strategy. For example, because of the degradation cost modeling, a small difference occurs at 8:15 in comparison with Case 2 when HESS in Case 2 discharges over 2 kW electricity to the H-MG, and HESS in Case 6 does not take any action, which causes the H-MG to buy energy from the utility to afford the consumption at that time (shown in Figure 14c). That is because the RTP of utility is lower than the total discharging RTP of HESS with the quadratic model and higher than the total discharging RTP of HESS with the reciprocal model.

Another thing to note is that though the principle in the proposed strategy is the RTP of utility is lower than the total discharging RTP of HESS since the capacity of HESS is constant, HESS is not always dischargeable in every time slot that meets the requirement, such as the compliant time slot 7:15 in both Case 2 and Case 6.

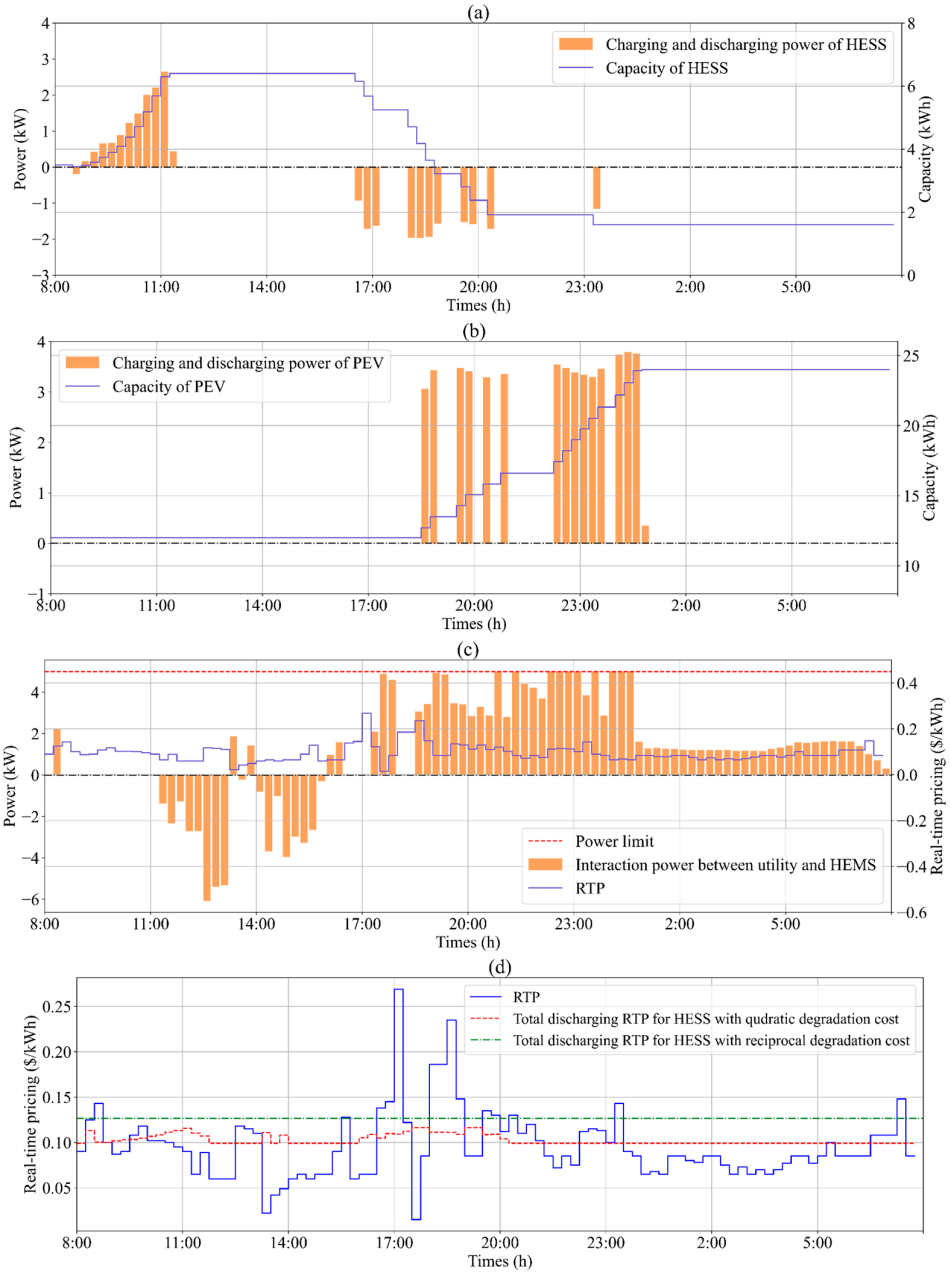


Figure 14. Load profiles for (**a**) HESS in HESS2H mode, (**b**) PEV in G2V mode, (**c**) H-MG without mode segmentation strategy, and (**d**) RTP comparison of HESS considering degradation cost.

In Case 7, all the household appliances, HESS, and PEV are in the same mode as Case 3. Slight growth of the degradation cost from 0.4923 USD/day to 0.4988 USD/day seen from Table 4 matches well with the discharging operation at 23:15 shown in Figure 15b since other compliant dischargeable time slots in Figure 15d are occupied by the HESS, which can be seen in Figure 15a. The cost of electricity and total cost are reduced up to 75.34% and 82.22%, respectively, compared with Case 1 and Case 5, and the load profile of the H-MG is presented in Figure 15c.

In Case 8, the energy cost and the total cost are 2.7600 and 3.2588 USD/day, which are a 29.19% and 22.01% descent, respectively, compared to Case 5. Compared with Case 4, HESS in Case 8 presents a longer discharging process, as shown in Figure 16a, and the PEV in Case 8 has fewer discharging behaviors, while the charging operation is shifted to the early morning, too, as shown in Figure 16b.

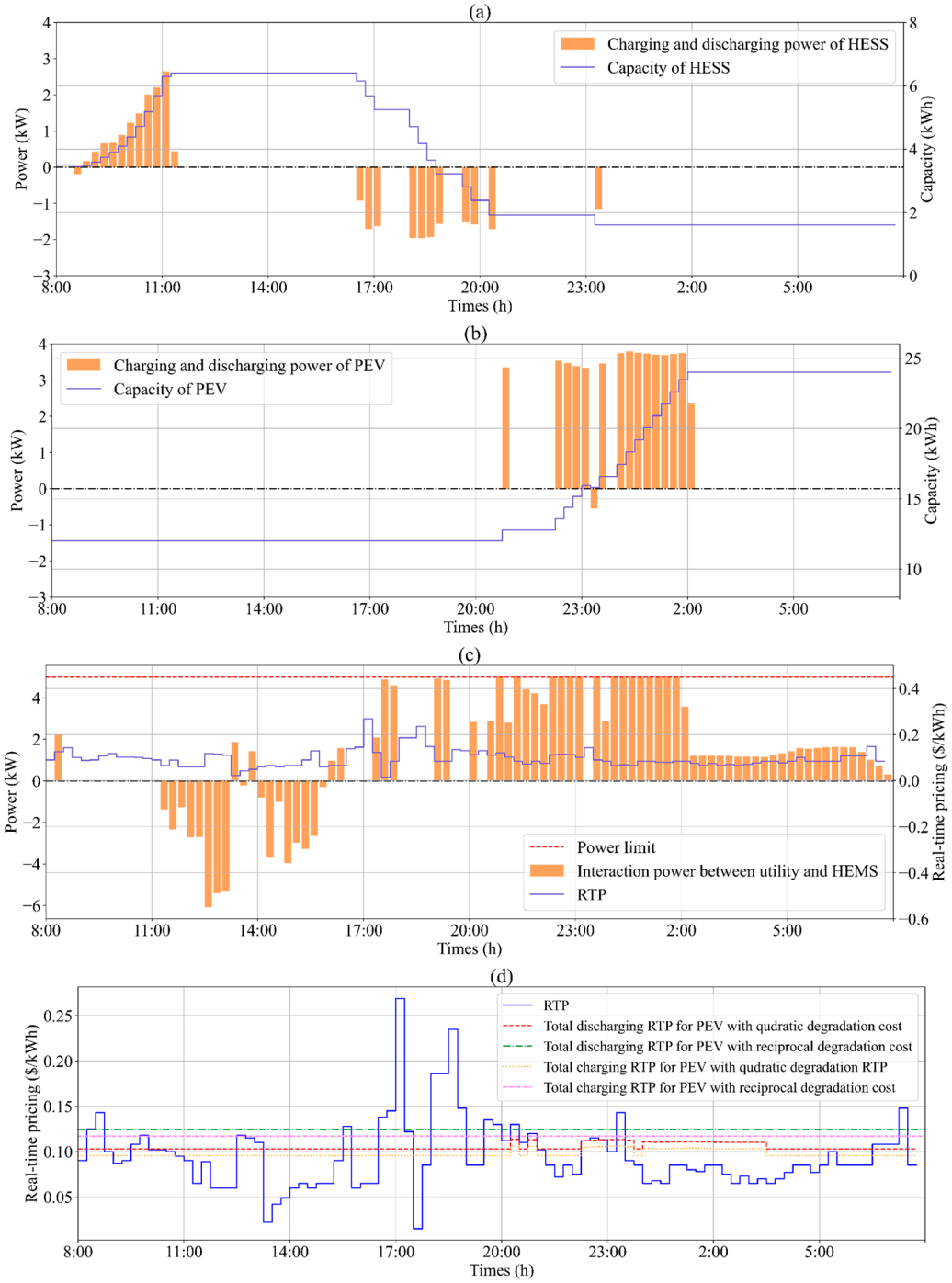


Figure 15. Load profiles for (**a**) HESS in HESS2H mode, (**b**) PEV in V2H mode, (**c**) H-MG without mode segmentation strategy, and (**d**) RTP comparison of PEV considering degradation cost.

It should be noted that due to the degradation price of batteries in the quadratic degradation cost model being dynamically related to the charging and discharging power changes of batteries, the total charging and discharging RTP of PEV also have the same relationship with the power changes of batteries, which causes the total charging and discharging RTP of PEV in Case 8 to be higher than in Case 7. Meanwhile, the total charging and discharging RTP of PEV in the reciprocal degradation cost model are fixed. So, after scheduling and load shifting by the proposed strategy, Case 8 shows a higher magnitude of cost reduction from 75.34% to 70.81%, compared with Case 4, from 69.58% to 69.16%.

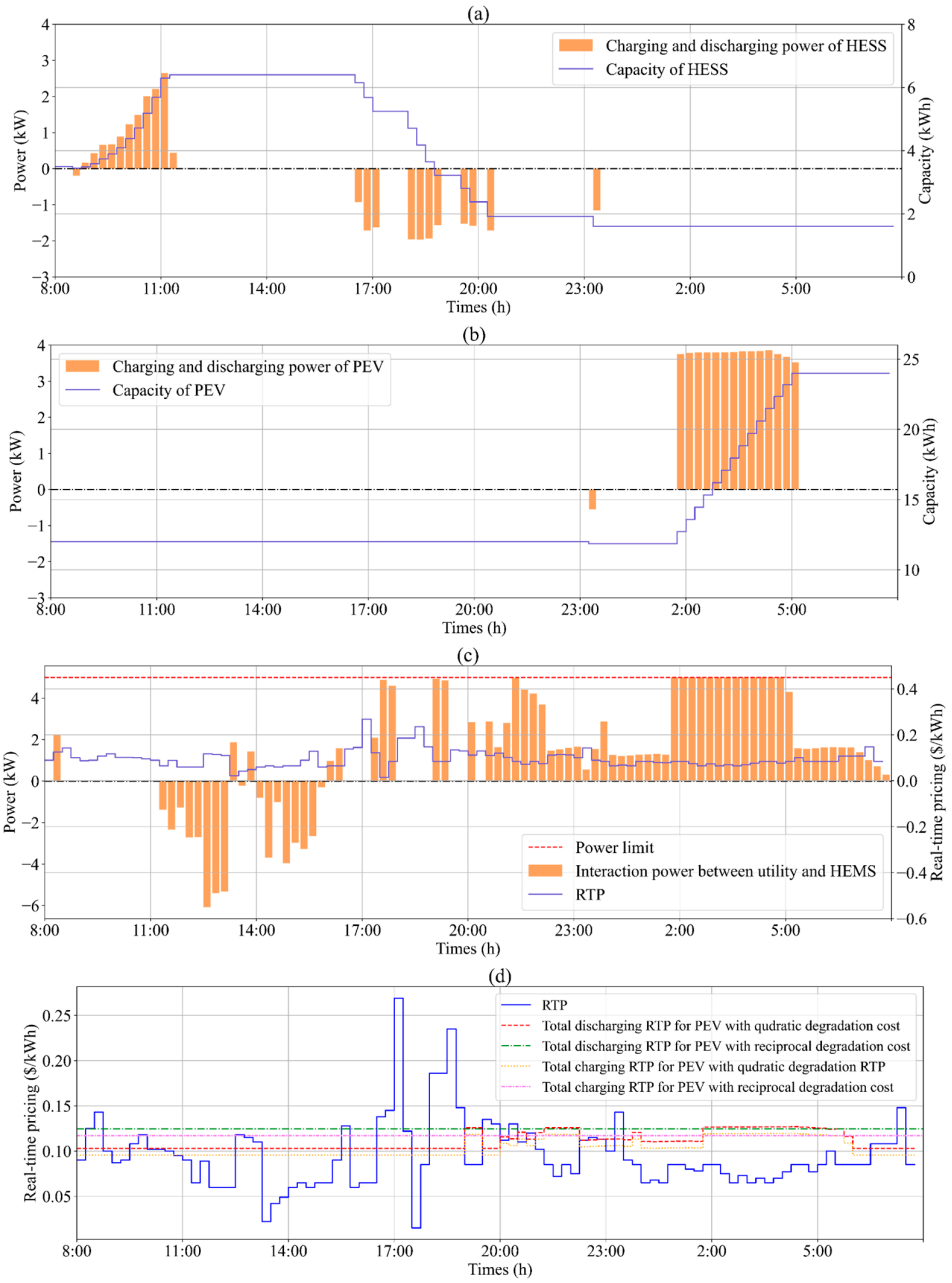


Figure 16. Load profiles for (**a**) HESS in HESS2H mode, (**b**) PEV in V2H mode, (**c**) H-MG combined mode segmentation strategy, and (**d**) RTP comparison of PEV considering degradation cost.

4.3. Sensitivity Analysis

Since the proposed charging and discharging strategy is based on the total discharging RTP of HESS and PEV considering the degradation cost of a battery, sensitivity analysis on the total discharging RTP of HESS and PEV with two degradation cost models are made, respectively, to analyze their impact on the electricity cost and assess the robustness of the proposed algorithm. In this paper, the discharging RTP of both HESS and PEV are set to increase from 0.1 times RTP_{AVG} to 4 times RTP_{AVG}, and the step length is set to 0.01 times RTP_{AVG}. Figure 17a shows the impact of the HESS discharging pricing threshold on the electricity cost in quadratic and reciprocal degradation cost models separately. The figures indicate whenever the discharging RTP of HESS is too low, which can make HESS release the stored energy of the battery in the low-price periods, or too high, which can reduce the dischargeable time of HESS, the electricity cost would increase accordingly. Additionally, if the discharging RTP of HESS is higher or lower than the highest and lowest

RTP, HESS cannot discharge to the H-MG at any time slot. To get the best solution and compare the impact of the two degradation cost models, the discharging RTP of HESS is set to 1.04 times RTP_{AVG} in this paper. Similar to HESS, Figure 17b shows the impact of the PEV discharging pricing threshold on the electricity cost in quadratic and reciprocal degradation cost models separately. However, due to the narrow area of best solutions, the parameter of PEV discharging RTP is not able to match, so the discharging RTP of HESS is set to 1.08 times RTP_{AVG} to satisfy both models and obtain a suboptimal solution.

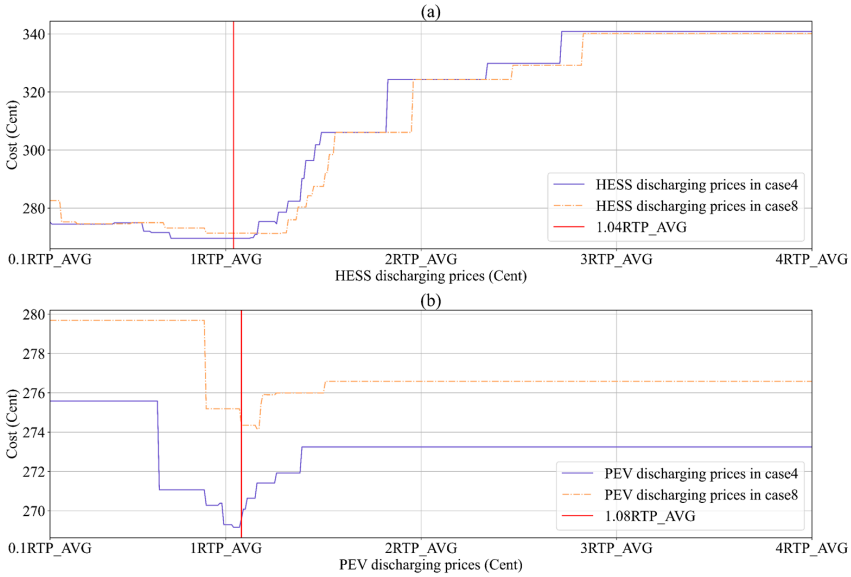


Figure 17. The impact of the discharge RTP threshold on the electricity cost for (**a**) HESS and (**b**) PEV.

4.4. Modeling Error Analysis

As discussed in Section 4.2, parameters of γ and θ are chosen based on the same sum of the degradation cost to get the same baseline of this case study, which is presented in Figure 18a. However, with the combination of HESS and the increasing charging and discharging behavior of both HESS and PEV, error occurs in the cases, such as Case 4 and Case 8 shown in Figure 18b.

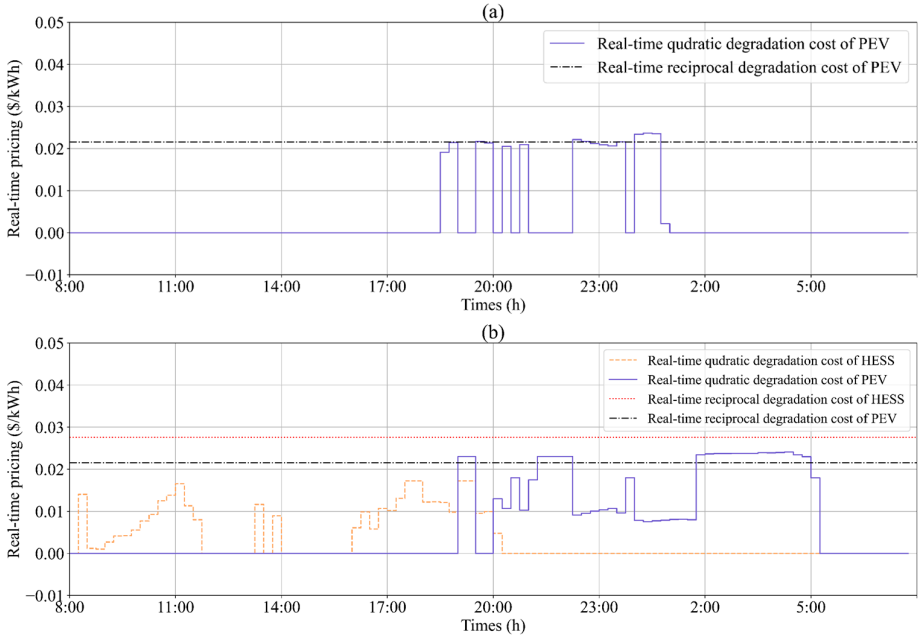


Figure 18. RTP comparison of degradation cost for (**a**) Case 1 vs. Case 5 and (**b**) Case 4 vs. Case 8.

Specifically, though the sum of the degradation cost of PEV in Case 8 is still similar to the value in Case 4, the real-time degradation cost of HESS in the quadratic model is always lower than the cost in the reciprocal model. Fortunately, since this error is very small compared to the total cost, it is not of much concern. In addition, this condition can be eliminated in a future study when taking the degradation cost of HESS into the based case, too.

4.5. Other Findings and Limitations

The other findings and insights of this work are listed as follows:

- Installing HESS in the home leads to decreasing the cost of energy and making full use of the power generated by the PV panels;
- The change of the operation mode of PEV and the combination of the proposed charging and discharging strategy of batteries improve the efficiency of the PV-integrated HEMS and decrease the electricity cost and total cost;
- The addition of the degradation cost has an influence on the charging and discharging behavior of HESS and PEV batteries, and a fully equipped HEMS with a suitable degradation cost model (Case 4) leads to the best optimization plan between the cases.

The limitations of the work are listed as follows:

- It is assumed that the everyday arrival and departure time of PEV are fixed in this study, which cannot be reached in reality, and the uncertainty of the arrival and departure time of PEV can be taken into account in the future simulations;
- The quadratic model of degradation cost is simple to calculate but does not consider the investment cost of batteries, which can affect the results of simulations;
- The investment cost of batteries is included in the reciprocal degradation cost model; however, the parameters of batteries for HESS and PEV are assumed to be fixed in this work, which are, in fact, changeable during the daily use of HESS and PEV and can slightly change the results;
- The selling price of energy is assumed to be 50% of the buying price of the utility. In reality, the selling price of energy is not always related to the buying price of the utility and is often affected by the financial incentives proposed by utilities.

5. Conclusions

In this study, an MIP-based HEMS architecture and its scheduling strategy is proposed to minimize the daily energy cost in H-MG and satisfy residents' thermal comfort in daily life. As one of its main contributions, this study combines and satisfies the users' comfort requirements of both AC and EWH in the framework. The installation of HESS in the home not only makes full use of the power generated by the PV panels but also decrease the cost of electricity. The proposed algorithm classifies and schedules household appliances into three types (EA, CA, and SA) according to the electrical performance of appliances and user preferences. By combining the novel mode segmentation charging and discharging strategy for the batteries of HESS and PEV, the effectiveness of the HEMS and the impact of the modeling of battery degradation are investigated, taking into account the impact of real-time pricing, two types of models of battery degradation cost, and technical constraints of appliances, which not only guarantee the lowest cost and users' comfort but also manage the energy transaction reasonably between the residence and utility and prolongs the service life of the batteries. The results of our case study show the highest daily electricity cost and total cost reduction of 30.84% (from 3.8978 USD/day to 2.6985 USD/day) and 24.16% (from 4.1786 USD/day to 3.1692 USD/day), respectively, in Case 4. The proposed mode segmentation strategy to control the charging and discharging operation of HESS and PEV also presents the ability to prolong the service life of the battery by separating the charging and discharging behavior of PEV into two modes and shifting the charging process of PEV to the lower RTP time period. Sensitivity analysis and modeling error analysis indicate the robustness and developability of the proposed energy management system.

Author Contributions: Conceptualization, B.H. and Y.Z.; Methodology, Y.Z.; Software, B.H. and Y.Z.; Validation, B.H. and Y.Z.; Writing—original draft, B.H. and Y.Z.; Writing—review & editing, B.H. and Y.Z.; Visualization, A.S.; Supervision, M.M., S.M., M.S. and A.S. All authors have read and agreed to the published version of the manuscript.

Funding: The authors would like to thank the Ministry of Higher Education, Malaysia, for providing financial support under the Large Research Grant Scheme (LRGS): LRGS/1/2019/UKM/01/6/3 and the Universiti Tenaga Nasional grant no. IC6-BOLDREFRESH2025 (HCR) under the BOLD2025 Program.

Data Availability Statement: Not applicable.

Conflicts of Interest: The authors declare no conflict of interest.

Nomenclature

Abbreviations

AC	Air conditioning
CA	Constrained appliance
CPP	Critical peak pricing
DR	Demand response
EA	Entertainment appliance
EWH	Electric water heater
G2V	Grid-to-vehicle
HEMS	Home energy management system
HESS	Home energy storage system
HESS2H	HESS-to-home
H-MG	Home micro-grid
IBR	Inclining block rates
MIP	Mixed integer programming
PAR	Peak-to-average ratio
PEV	Plug-in electric vehicle
PV	Photovoltaic
RESs	Renewable energy sources
SA	Schedulable appliance
SG	Smart grid
TOU	Time-of-use
V2H	Vehicle-to-home

Sets and indices

T	Set of time slots
t	Index of time slots
S	Set of SA loads
s	Index of SA loads

Parameters

A_{PV}	PV surface area
C_{HESS}^{max}	Maximum capacity of the batteries used in HESS (kWh)
C_{HESS}^{int}	Initial capacity of the batteries used in HESS (kWh)
Cyc_{HESS}	Lifetime in cycles of the batteries used in HESS
C_{PEV}^{max}	Maximum capacity of the batteries used in PEV (kWh)
C_{PEV}^{int}	Initial capacity of the batteries used in PEV (kWh)
Cyc_{PEV}	Lifetime in cycles of the batteries used in PEV
DoD_{HESS}	Depth of discharge of the batteries used in HESS (%)
DoD_{PEV}	Depth of discharge of the batteries used in PEV (%)
num_{load}	Number of time intervals that appliances need to fulfill their tasks
P_E	Power consumption of EA loads (kW)
P_{DR}	Maximum power drawn from the utility (kW)
p_{HESS}^{chmax}	Maximum charging power of the batteries used in HESS (kW)
p_{HESS}^{dismax}	Maximum discharging power of the batteries used in HESS (kW)
P_{load}	Power of the load
p_{PEV}^{chmax}	Maximum charging power of the batteries used in PEV (kW)

P_{PEV}^{dismax}	Maximum discharging power of the batteries used in PEV (kW)
P_{PV}	PV generation (kW)
Q	Energy input rate
Q_{sun}	Solar irradiance
Rep_{HESS}	Replacement cost including labor of the batteries used in HESS ($)
Rep_{PEV}	Replacement cost including labor of the batteries used in PEV ($)
RTP	Real − time pricing ($/kWh)
RTP_{AVG}	Average real − time pricing ($)
RTP_{HESS}^{dis}	Real-time discharging pricing of the batteries used in HESS
RTP_{PEV}^{ch}	Real-time charging pricing of the batteries used in PEV
RTP_{PEV}^{dis}	Real-time discharging pricing of the batteries used in PEV
S_C	Surface coefficient
T^{cw}	Incoming cold water temperature (°F)
T^{en}	Ambient temperature (°F)
T^{out}	Outdoor temperature (°F)
T_{AC}^{max}	Maximum acceptable indoor temperature of user (°F)
T_{AC}^{min}	Minimum acceptable indoor temperature of user (°F)
T_{AC}^{int}	Initial indoor temperature (°F)
T_{EWH}^{max}	Maximum acceptable hot water temperature of user (°F)
T_{EWH}^{min}	Minimum acceptable hot water temperature of user (°F)
T_{EWH}^{int}	Initial water temperature (°F)
t_a	Arrival time of PEV
t_d	Departure time of PEV
t_{load}^{start}	Start time of the load
t_{load}^{end}	End time of the load
Δt	Time interval (15 min)
α, β	Thermal characteristics of air conditioning
η_{HESS}^{ch}, η_{HESS}^{dis}	Charging and discharging efficiency of the batteries used in HESS
η_{PEV}^{ch}, η_{PEV}^{dis}	Charging and discharging efficiency of the batteries used in PEV
η_{PV}	Efficiency of PV
Variables	
C_{HESS}	Capacity of the batteries used in HESS (kWh)
$\cos t_{HESS,\,PEV}^{deg}$	Degradation cost of HESS and PEV
C_{PEV}	Capacity of the batteries used in PEV (kWh)
P_{AC}	Power of air conditioning (kW)
P_{EWH}	Power of electric water heater (kW)
P_G	The interaction power between the utility and H-MG (kW)
P_{HESS}	Power of HESS (kW)
P_{HESS}^{ch}	Charging power of HESS (kW)
P_{HESS}^{chable}	Maximum chargeable power of HESS (kW)
P_{HESS}^{dis}	Discharging power of HESS (kW)
$P_{HESS}^{disable}$	Maximum dischargeable power of HESS (kW)
P_{PEV}	Power of PEV (kW)
P_{PEV}^{ch}	Charging power of PEV (kW)
P_{PEV}^{chable}	Maximum chargeable power of PEV (kW)
P_{PEV}^{dis}	Discharging power of PEV (kW)
$P_{PEV}^{disable}$	Maximum dischargeable power of PEV (kW)
T^{in}	Indoor temperature (°F)
T^{hw}	Hot water temperature (°F*r*)
u_d	Running state of SA loads (binary variable: 1 for charging and 0 for discharging)
u_{HESS}	Running state of HESS (binary variable: 1 for charging and 0 for discharging)
u_{PEV}	Running state of PEV (binary variable: 1 for charging and 0 for discharging)

References

1. Han, B.; Zahraoui, Y.; Mubin, M.; Mekhilef, S.; Seyedmahmoudian, M.; Stojcevski, A. Home Energy Management Systems : A Review of the Concept, Architecture, and Scheduling Strategies. *IEEE Access* **2023**, *11*, 19999–20025. [CrossRef]
2. Zahraoui, Y.; Alhamrouni, I.; Mekhilef, S.; Reyasudin Basir Khan, M.; Seyedmahmoudian, M.; Stojcevski, A.; Horan, B. Energy management system in microgrids: A comprehensive review. *Sustainability* **2021**, *13*, 10492. [CrossRef]
3. Hou, Q.; Zhang, N.; Du, E.; Miao, M.; Peng, F.; Kang, C. Probabilistic duck curve in high PV penetration power system: Concept, modeling, and empirical analysis in China. *Appl. Energy* **2019**, *242*, 205–215. [CrossRef]
4. Zahraoui, Y.; Alhamrouni, I.; Basir Khan, M.R.; Mekhilef, S.; Hayes, B.P.; Rawa, M.; Ahmed, M. Self-healing strategy to enhance microgrid resilience during faults occurrence. *Int. Trans. Electr. Energy Syst.* **2021**, *31*, 13232. [CrossRef]
5. International Energy Agency (IEA) World Energy Balances. 2022. Available online: https://www.iea.org/data-and-statistics/data-tools/energy-statistics-data-browser?country=WORLD&fuel=Energyconsumption&indicator=ElecConsBySector (accessed on 26 January 2023).
6. Elkazaz, M.; Sumner, M.; Pholboon, S.; Davies, R.; Thomas, D. Performance assessment of an energy management system for a home microgrid with PV generation. *Energies* **2020**, *13*, 3436. [CrossRef]
7. Samadi, A.; Saidi, H.; Latify, M.A.; Mahdavi, M. Home energy management system based on task classification and the resident's requirements. *Int. J. Electr. Power Energy Syst.* **2020**, *118*, 105815. [CrossRef]
8. Luo, J.T.; Joybari, M.M.; Panchabikesan, K.; Sun, Y.; Haghighat, F.; Moreau, A.; Robichaud, M. Performance of a self-learning predictive controller for peak shifting in a building integrated with energy storage. *Sustain. Cities Soc.* **2020**, *60*, 102285. [CrossRef]
9. Javadi, M.S.; Gough, M.; Lotfi, M.; Esmaeel Nezhad, A.; Santos, S.F.; Catalão, J.P.S. Optimal self-scheduling of home energy management system in the presence of photovoltaic power generation and batteries. *Energy* **2020**, *210*, 118568. [CrossRef]
10. Duman, A.C.; Erden, H.S.; Gönül, Ö.; Güler, Ö. A home energy management system with an integrated smart thermostat for demand response in smart grids. *Sustain. Cities Soc.* **2021**, *65*, 102639. [CrossRef]
11. Beaudin, M.; Zareipour, H. Home energy management systems: A review of modelling and complexity. *Renew. Sustain. Energy Rev.* **2015**, *45*, 318–335. [CrossRef]
12. Moen, R.L. Solar Energy Management System. In Proceedings of the Proceedings of the IEEE Conference on Decision and Control, Fort Lauderdale, FL, USA, 12–14 December 1979; Volume 2, pp. 917–919.
13. Zahraoui, Y.; Alhamrouni, I.; Mekhilef, S.; Basir Khan, M.R.; Hayes, B.P.; Ahmed, M. A novel approach for sizing battery storage system for enhancing resilience ability of a microgrid. *Int. Trans. Electr. Energy Syst.* **2021**, *31*, e13142. [CrossRef]
14. Alsharif, A.; Tan, C.W.; Ayop, R.; Dobi, A.; Lau, K.Y. A comprehensive review of energy management strategy in Vehicle-to-Grid technology integrated with renewable energy sources. *Sustain. Energy Technol. Assess.* **2021**, *47*, 101439. [CrossRef]
15. Ben Arab, M.; Rekik, M.; Krichen, L. Suitable various-goal energy management system for smart home based on photovoltaic generator and electric vehicles. *J. Build. Eng.* **2022**, *52*, 104430. [CrossRef]
16. Capehart, B.L.; Muth, E.J.; Storin, M.O. Minimizing residential electrical energy costs using microcomputer energy management systems. *Comput. Ind. Eng.* **1982**, *6*, 261–269. [CrossRef]
17. Hensgen, D.A.; Kidd, T.; St. John, D.; Schnaidt, M.C.; Siegel, H.J.; Braun, T.D.; Maheswaran, M.; Ali, S.; Kim, J.K.; Irvine, C.; et al. An overview of MSHN: The management system for heterogeneous networks. In Proceedings of the Heterogeneous Computing Workshop, Washington, DC, USA, 12 April 1999; pp. 184–198.
18. Tostado-Véliz, M.; Gurung, S.; Jurado, F. Efficient solution of many-objective Home Energy Management systems. *Int. J. Electr. Power Energy Syst.* **2022**, *136*, 107666. [CrossRef]
19. Gholami, M.; Sanjari, M.J. Multiobjective energy management in battery-integrated home energy systems. *Renew. Energy* **2021**, *177*, 967–975. [CrossRef]
20. Merdanoğlu, H.; Yakıcı, E.; Doğan, O.T.; Duran, S.; Karatas, M. Finding optimal schedules in a home energy management system. *Electr. Power Syst. Res.* **2020**, *182*, 106229. [CrossRef]
21. Mansouri, S.A.; Ahmarinejad, A.; Nematbakhsh, E.; Javadi, M.S.; Jordehi, A.R.; Catalão, J.P.S. Energy management in microgrids including smart homes: A multi-objective approach. *Sustain. Cities Soc.* **2021**, *69*, 102852. [CrossRef]
22. Mak, D.; Choi, D.H. Optimization framework for coordinated operation of home energy management system and Volt-VAR optimization in unbalanced active distribution networks considering uncertainties. *Appl. Energy* **2020**, *276*, 115495. [CrossRef]
23. Lu, Q.; Zhang, Z.; Lü, S. Home energy management in smart households: Optimal appliance scheduling model with photovoltaic energy storage system. *Energy Rep.* **2020**, *6*, 2450–2462. [CrossRef]
24. Shakeri, M.; Shayestegan, M.; Reza, S.M.S.; Yahya, I.; Bais, B.; Akhtaruzzaman, M.; Sopian, K.; Amin, N. Implementation of a novel home energy management system (HEMS) architecture with solar photovoltaic system as supplementary source. *Renew. Energy* **2018**, *125*, 108–120. [CrossRef]
25. Esmaeel Nezhad, A.; Rahimnejad, A.; Gadsden, S.A. Home energy management system for smart buildings with inverter-based air conditioning system. *Int. J. Electr. Power Energy Syst.* **2021**, *133*, 107230. [CrossRef]
26. Javadi, M.S.; Nezhad, A.E.; Gough, M.; Lotfi, M.; Anvari-Moghaddam, A.; Nardelli, P.H.J.; Sahoo, S.; Catalão, J.P.S. Conditional Value-at-Risk Model for Smart Home Energy Management Systems. *e-Prime* **2021**, *1*, 100006. [CrossRef]
27. Langer, L.; Volling, T. An optimal home energy management system for modulating heat pumps and photovoltaic systems. *Appl. Energy* **2020**, *278*, 115661. [CrossRef]

28. Younes, Z.; Alhamrouni, I.; Mekhilef, S.; Reyasudin, M. A memory-based gravitational search algorithm for solving economic dispatch problem in micro-grid. *Ain Shams Eng. J.* **2021**, *12*, 1985–1994. [CrossRef]
29. Zupančič, J.; Filipič, B.; Gams, M. Genetic-programming-based multi-objective optimization of strategies for home energy-management systems. *Energy* **2020**, *203*, 117769. [CrossRef]
30. Mehrjerdi, H. Peer-to-peer home energy management incorporating hydrogen storage system and solar generating units. *Renew. Energy* **2020**, *156*, 183–192. [CrossRef]
31. Park, H. Human comfort-based-home energy management for demand response participation. *Energies* **2020**, *13*, 2463. [CrossRef]
32. Wang, X.; Mao, X.; Khodaei, H. A multi-objective home energy management system based on internet of things and optimization algorithms. *J. Build. Eng.* **2021**, *33*, 101603. [CrossRef]
33. Jin, X.; Baker, K.; Christensen, D.; Isley, S. Foresee: A user-centric home energy management system for energy efficiency and demand response. *Appl. Energy* **2017**, *205*, 1583–1595. [CrossRef]
34. Javadi, M.S.; Nezhad, A.E.; Nardelli, P.H.J.; Gough, M.; Lotfi, M.; Santos, S.; Catalão, J.P.S. Self-scheduling model for home energy management systems considering the end-users discomfort index within price-based demand response programs. *Sustain. Cities Soc.* **2021**, *68*, 102792. [CrossRef]
35. Bayram, I.S.; Ustun, T.S. A survey on behind the meter energy management systems in smart grid. *Renew. Sustain. Energy Rev.* **2017**, *72*, 1208–1232. [CrossRef]
36. Zahraoui, Y.; Korõtko, T.; Rosin, A.; Agabus, H. Market Mechanisms and Trading in Microgrid Local Electricity Markets: A Comprehensive Review. *Energies.* **2023**, *16*, 2145. [CrossRef]
37. Esther, B.P.; Kumar, K.S. A survey on residential Demand Side Management architecture, approaches, optimization models and methods. *Renew. Sustain. Energy Rev.* **2016**, *59*, 342–351. [CrossRef]
38. Sharifi, A.H.; Maghouli, P. Energy management of smart homes equipped with energy storage systems considering the PAR index based on real-time pricing. *Sustain. Cities Soc.* **2019**, *45*, 579–587. [CrossRef]
39. Ben Slama, S. Design and implementation of home energy management system using vehicle to home (H2V) approach. *J. Clean. Prod.* **2021**, *312*, 127792. [CrossRef]
40. Zahraoui, Y.; Alhamrouni, I.; Mekhilef, S.; Basir Khan, M.R. Chapter one—Machine learning algorithms used for short-term PV solar irradiation and temperature forecasting at microgrid. In *Applications of AI and IOT in Renewable Energy*; Shaw, R.N., Ghosh, A., Mekhilef, S., Balas, V.E., Eds.; Academic Press: Cambridge, MA, USA, 2022; pp. 1–17. ISBN 978-0-323-91699-8.
41. Zahraoui, Y.; Alhamrouni, I.; Hayes, B.P.; Mekhilef, S.; Korõtko, T. System-Level Condition Monitoring Approach for Fault Detection in Photovoltaic Systems. In *Fault Analysis and its Impact on Grid-connected Photovoltaic Systems Performance*; John Wiley & Sons, Ltd.: Hoboken, NJ, USA, 2022; pp. 215–254. ISBN 9781119873785.
42. Hou, X.; Wang, J.; Huang, T.; Wang, T.; Wang, P. Smart Home Energy Management Optimization Method Considering Energy Storage and Electric Vehicle. *IEEE Access* **2019**, *7*, 144010–144020. [CrossRef]
43. Li, N.; Chen, L.; Low, S.H. Optimal demand response based on utility maximization in power networks. In Proceedings of the 2011 IEEE Power and Energy Society General Meeting, Detroit, MI, USA, 24–28 July 2011.
44. Nehrir, M.H.; Jia, R.; Pierre, D.A.; Hammerstrom, D.J. Power management of aggregate electric water heater loads by voltage control. In Proceedings of the 2007 IEEE Power Engineering Society General Meeting, Tampa, FL, USA, 24–28 June 2007.
45. Liu, Y.; Li, Y.; Gooi, H.B.; Jian, Y.; Xin, H.; Jiang, X.; Pan, J. Distributed Robust Energy Management of a Multimicrogrid System in the Real-Time Energy Market. *IEEE Trans. Sustain. Energy* **2019**, *10*, 396–406. [CrossRef]
46. Khan, M.W.; Wang, J. Multi-agents based optimal energy scheduling technique for electric vehicles aggregator in microgrids. *Int. J. Electr. Power Energy Syst.* **2022**, *134*, 107346. [CrossRef]
47. The Australian Energy Market Operator (AEMO) Metadata. Available online: https://aemo.com.au/ (accessed on 27 October 2022).
48. Du, P.; Lu, N. Appliance commitment for household load scheduling. *IEEE Trans. Smart Grid* **2011**, *2*, 411–419. [CrossRef]

Disclaimer/Publisher's Note: The statements, opinions and data contained in all publications are solely those of the individual author(s) and contributor(s) and not of MDPI and/or the editor(s). MDPI and/or the editor(s) disclaim responsibility for any injury to people or property resulting from any ideas, methods, instructions or products referred to in the content.